Gravitational lensing constraints on the abundance of planetary & stellar mass PBHs

Anne Green

University of Nottingham, UK

1. Overview of (selected) new/updated constraints

2. Effect of PBH distribution on LMC microlensing constraints

1. overview of (selected) new/updated constraints

- LMC microlensing: OGLE long duration & high cadence
- supermagnified stars
- flux ratios of multiply lensed quasars

LMC microlensing

Stellar microlensing: temporary (achromatic) brightening of background star when compact object passes close to the line of sight. Paczynski

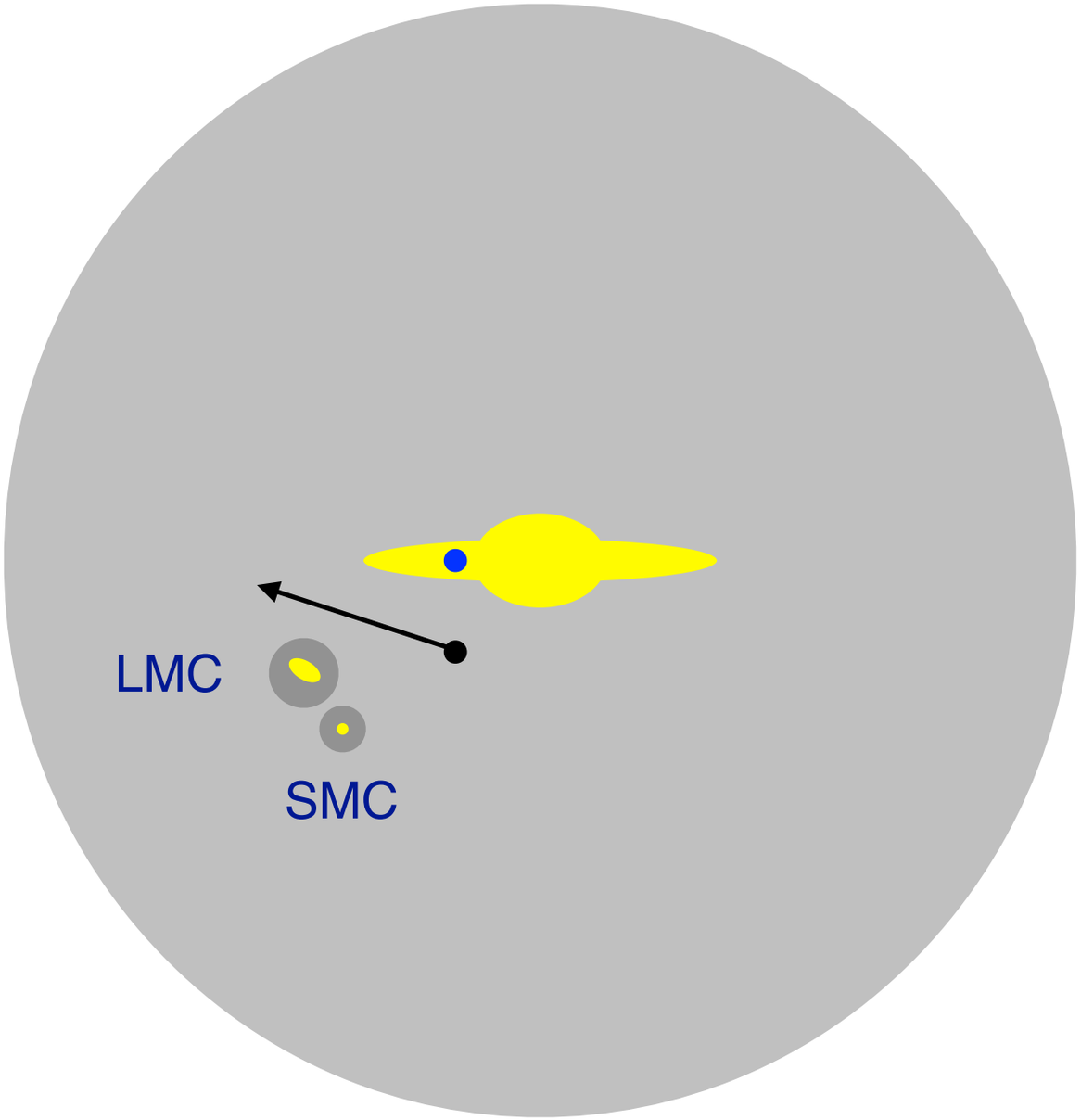

Not to scale!

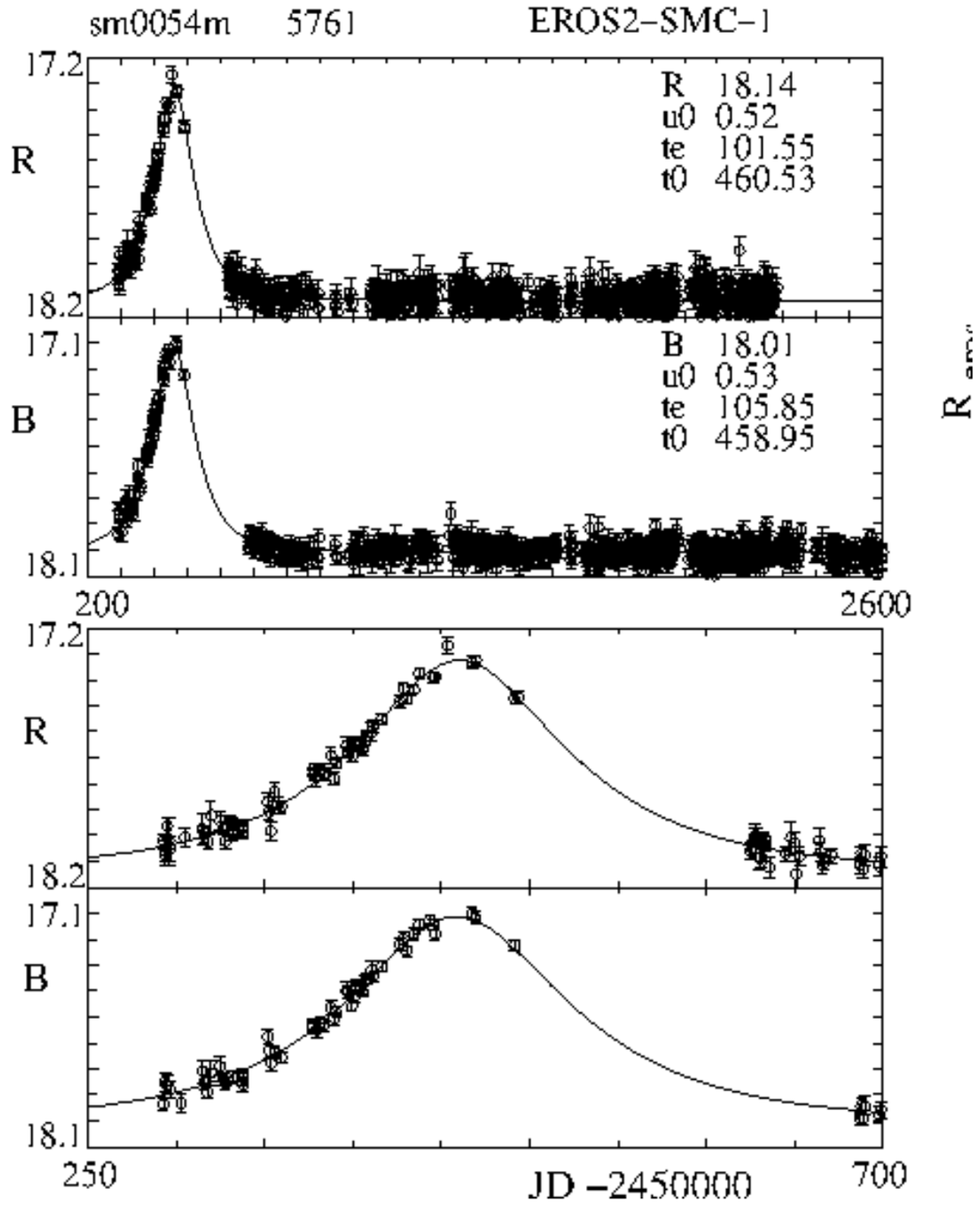

EROS

Einstein radius:

$$R_{\rm E}(x) = 2\left[\frac{GMx(1-x)L}{c^2}\right]^{1/2}$$

x = fractional distance along line of sight

along the line of sight

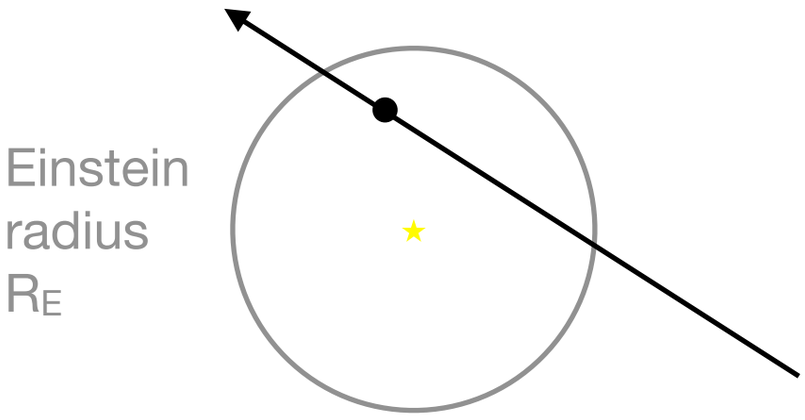

perpendicular to the line of sight

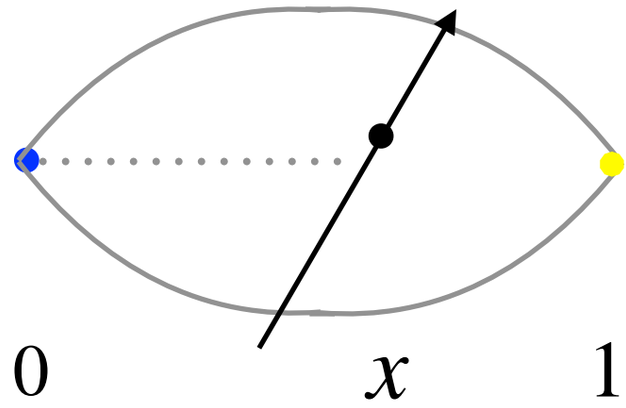

'Duration' of event (Einstein diameter* crossing time):

$$\hat{t} = \frac{2R_{\rm E}(x)}{v} \sim 1\,{\rm yr}\sqrt{x(1-x)}\left(\frac{M}{M_\odot}\right)^{1/2}$$

for source stars in LMC

* EROS & OGLE collaborations use Einstein radius crossing time

OGLE long duration

Observed ~80 million stars in LMC every (1-5) days for ~20 years: Mroz et al. arXiv:2403.02386

Observed 13 (+3) events with duration (Einstein radius crossing time) <1 year, no longer duration events.

Expect ~6 events from stars in LMC and ~(7-15) from stars in MW disk.

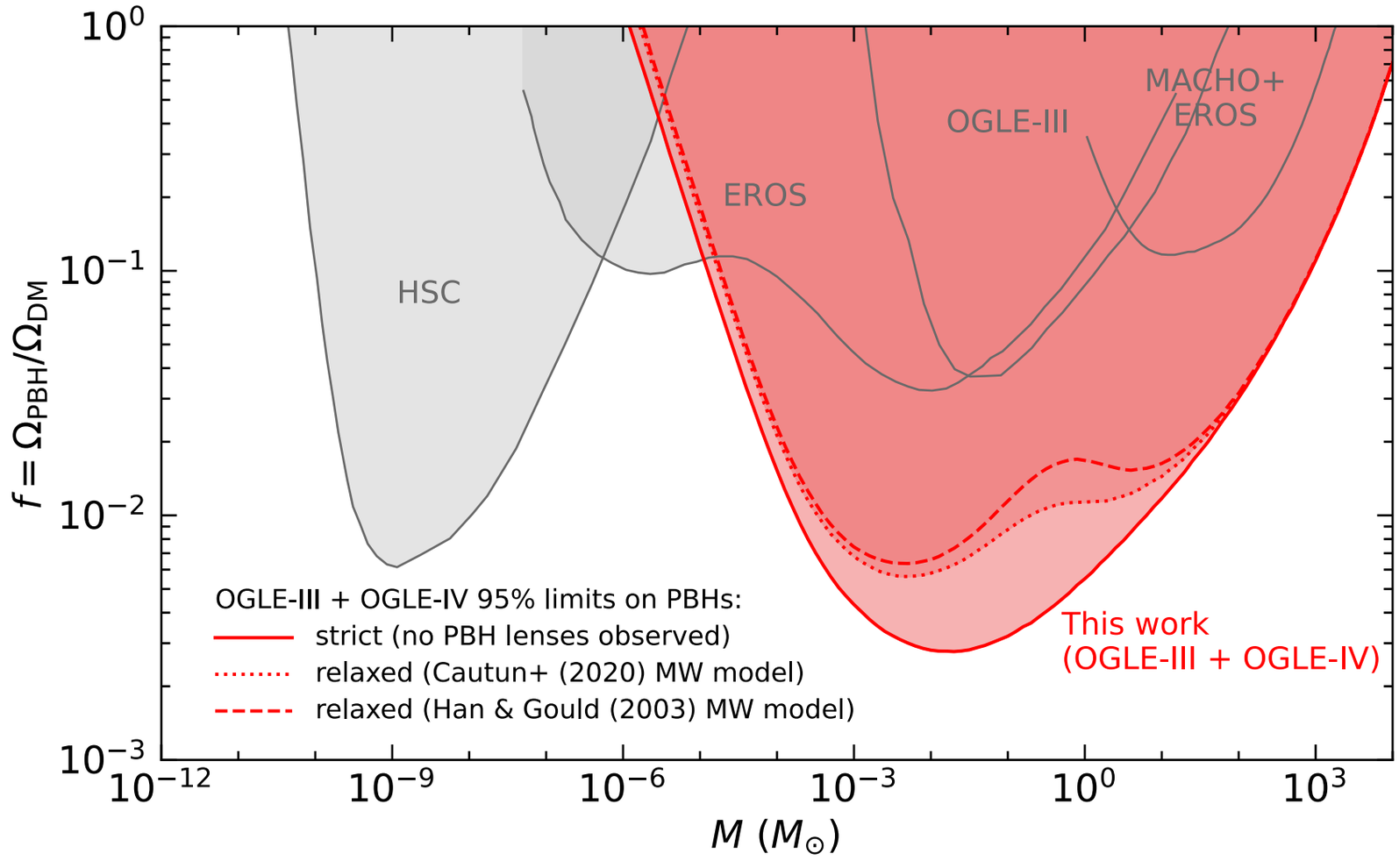

_____ strict (assumes all 13 events are due to stars/stellar remnants in LMC or MW disk)

…. & - - - - allow contribution from MW halo (2 different models for MW disk)

OGLE high cadence

Observed ~80 million stars in LMC every ~20 min for ~1 year: Mroz et al. arXiv:2410.06251

One candidate event. (taken ‘at face value’) inconsistent with PBH interpretation of ultra-short events towards Galactic bulge.

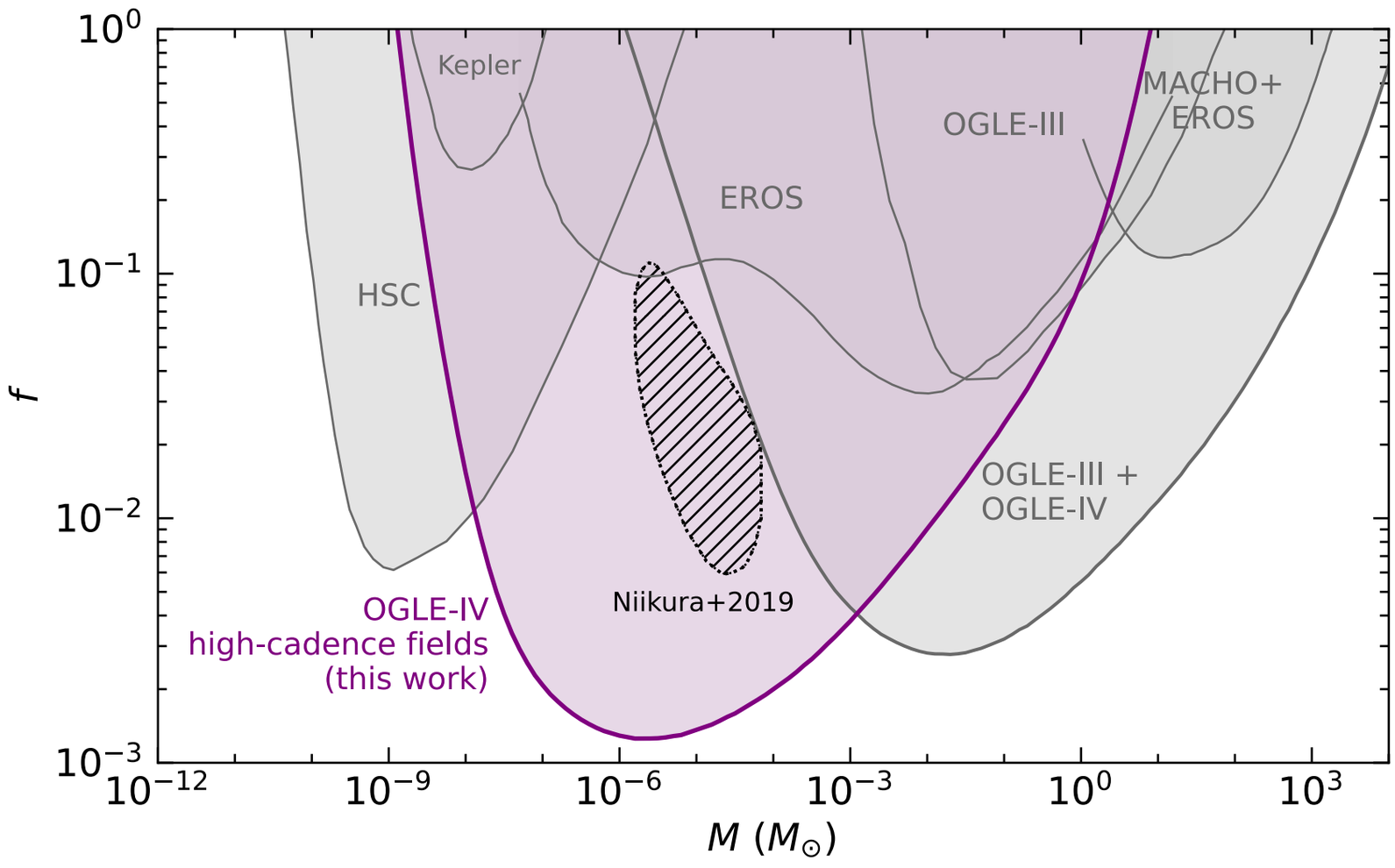

Compilation of stellar microlensing constraints

(under ‘standard’ assumptions, including a delta-function PBH mass function)

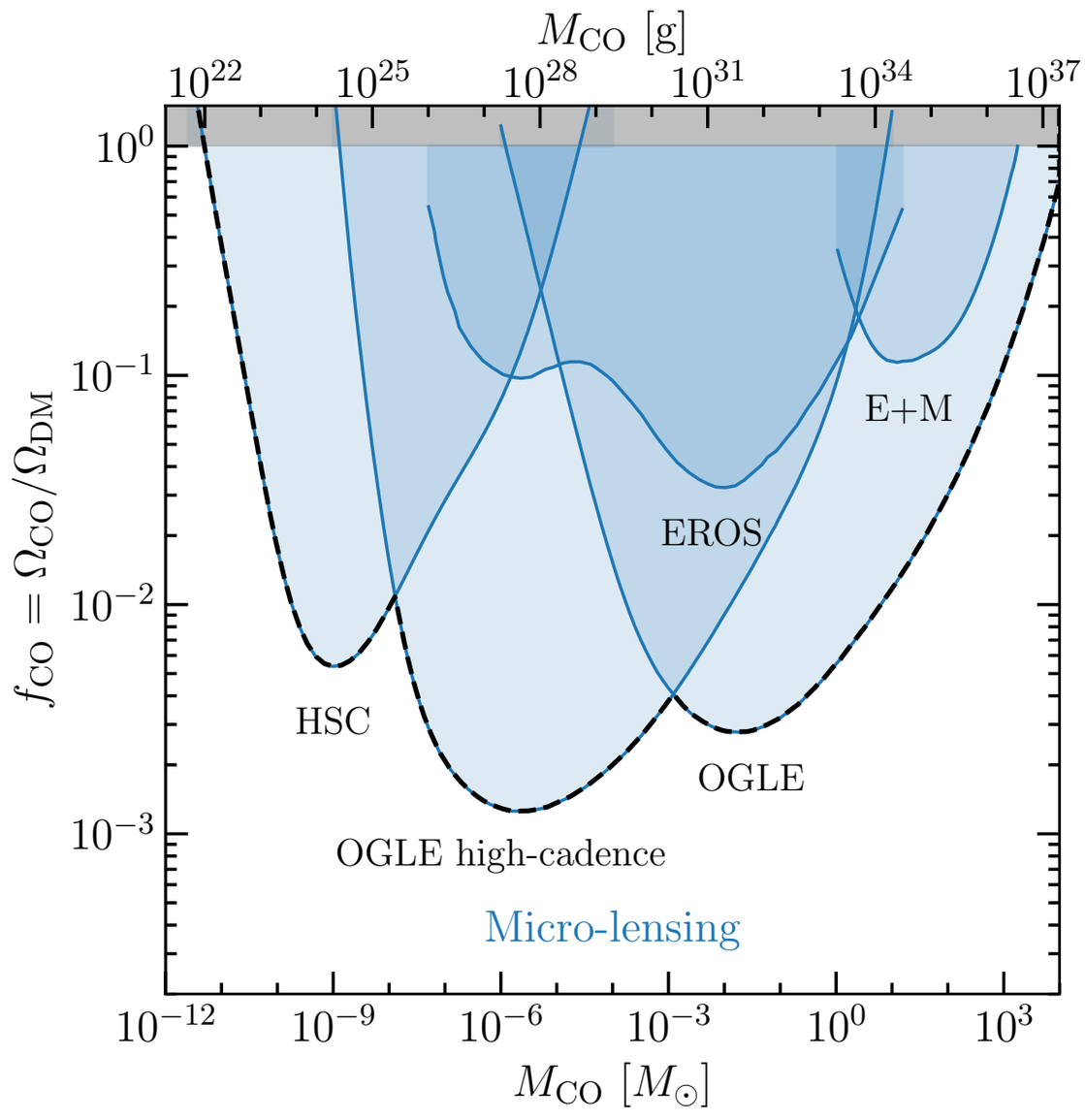

https://github.com/bradkav/PBHbounds

Supermagnified stars

When a distant star crosses a galaxy cluster caustic get huge magnification which can be increased by microlensing by compact objects (stars, stellar remnants, dark compact objects,..) in cluster. Miralda-Escude

However if large fraction of DM is in compact objects magnification is reduced.

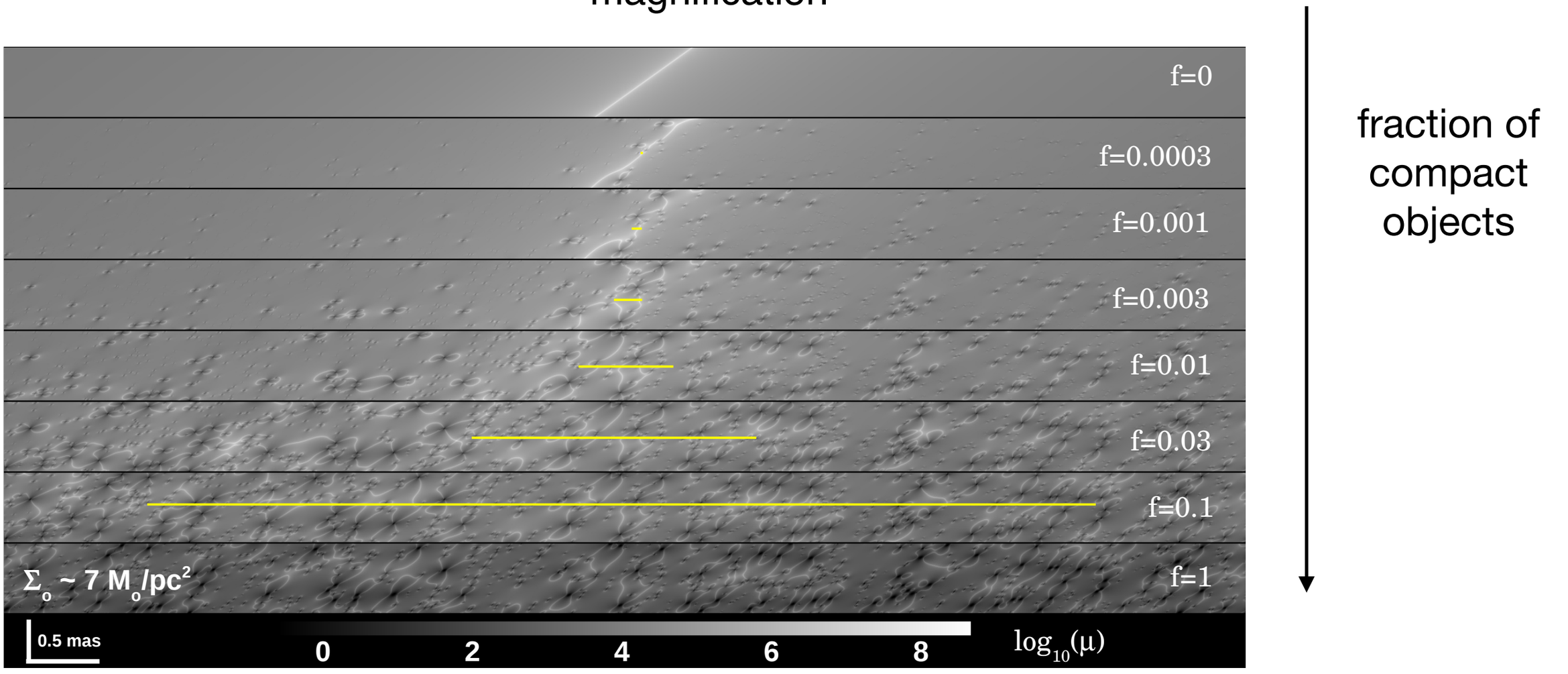

Kelly et al.

Supermagnified stars

When a distant star crosses a galaxy cluster caustic get huge magnification which can be increased by microlensing by compact objects (stars, stellar remnants, dark compact objects,..) in cluster. Miralda-Escude.

However if large fraction of DM is in compact objects magnification is reduced.

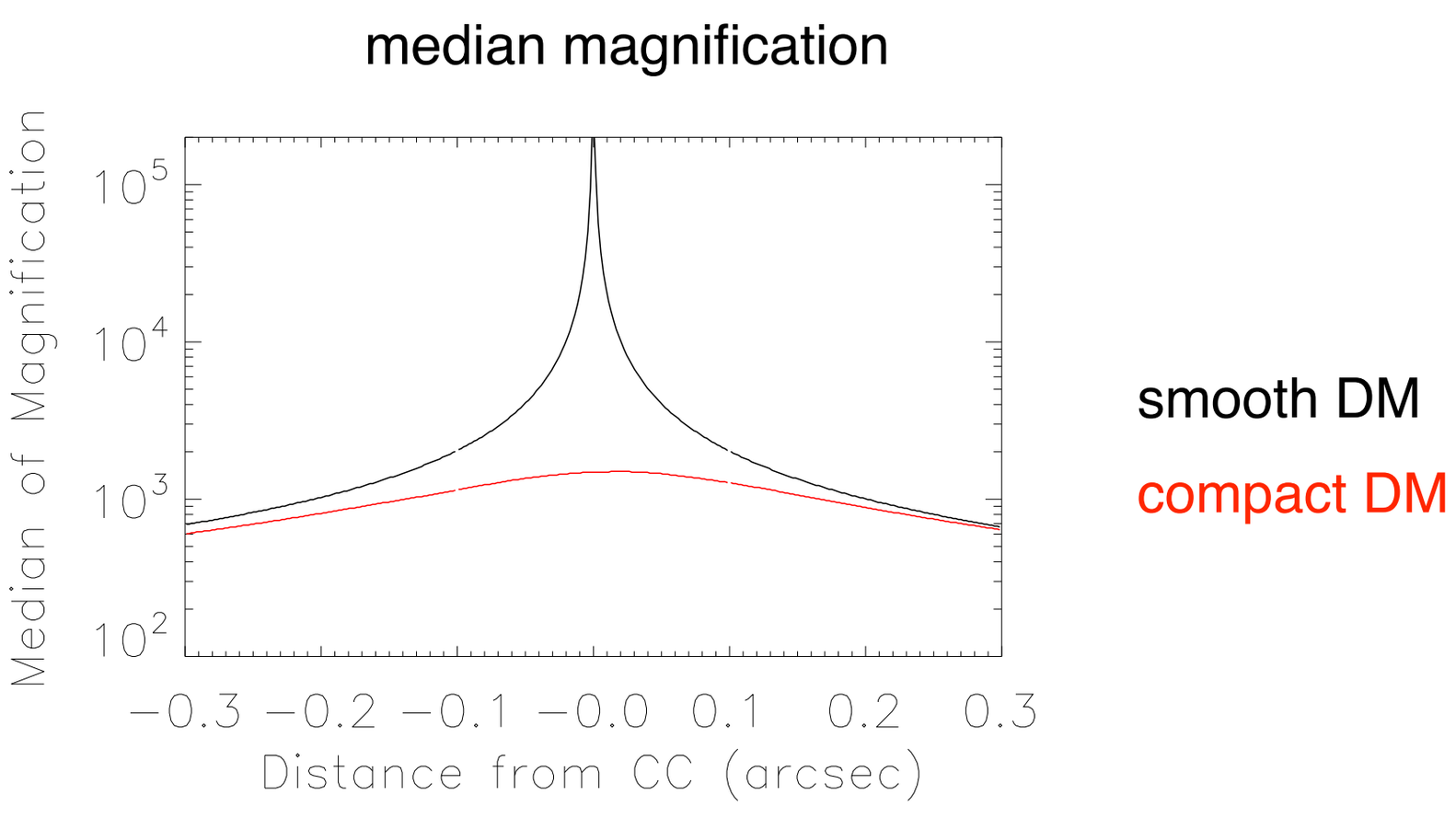

Kelly et al.

Icarus: star at red-shift 1.5, magnified x2000!, discovered serendipitously.

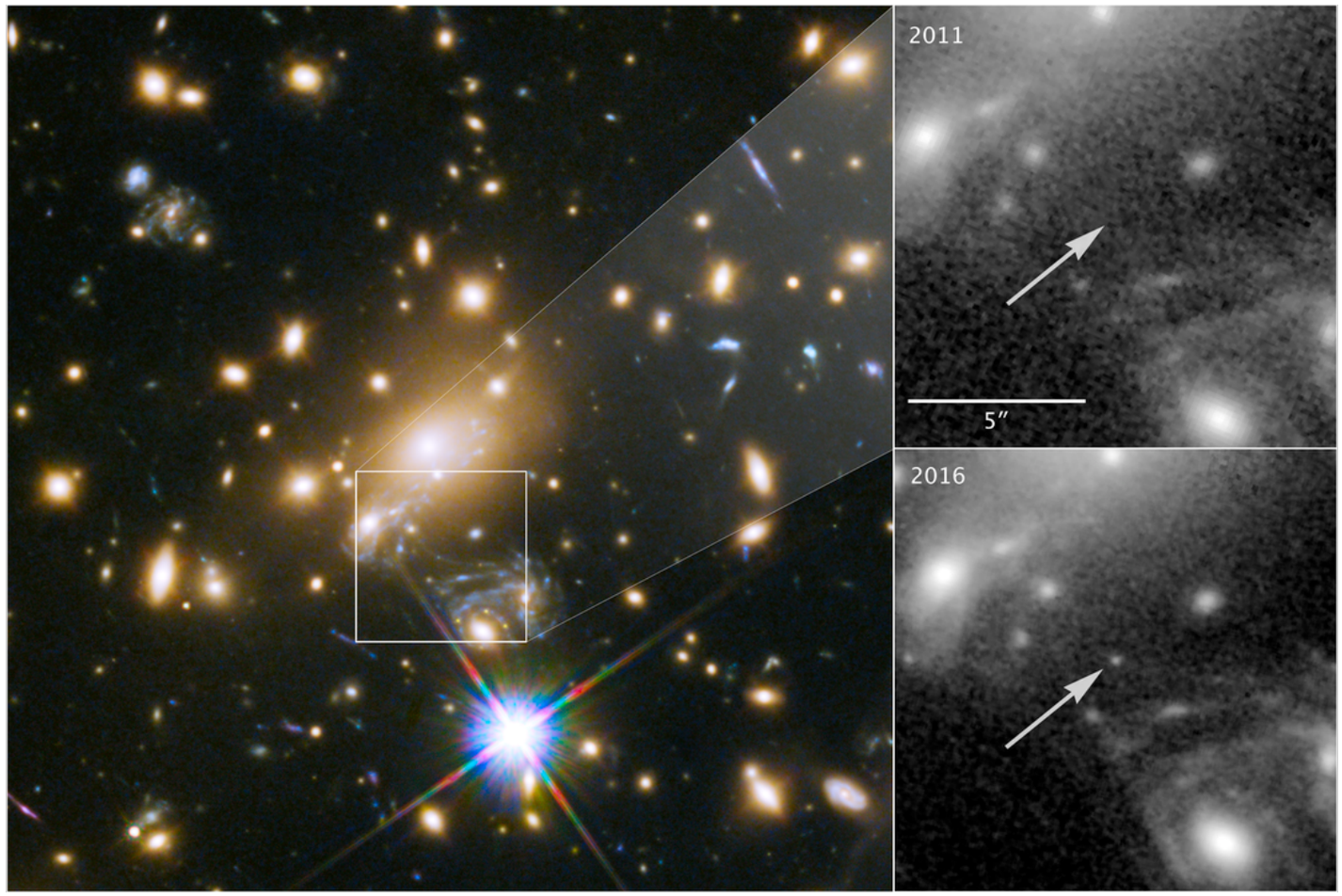

Kelly et al.

From positions of images of 9 supermagnified stars (Icarus, Warhol, Earendel, Mothra (at z=2.1),…): planetary mass and heavier compact objects make up less than ~3% of the dark matter. Vall Müller & Miradla-Escudé arXiv:2403.16989

Flux ratios of multiply-lensed quasars

Microlensing by compact objects in the lens galaxy leads to variations in the brightness of multiple-image quasars. Chang and Refsdal

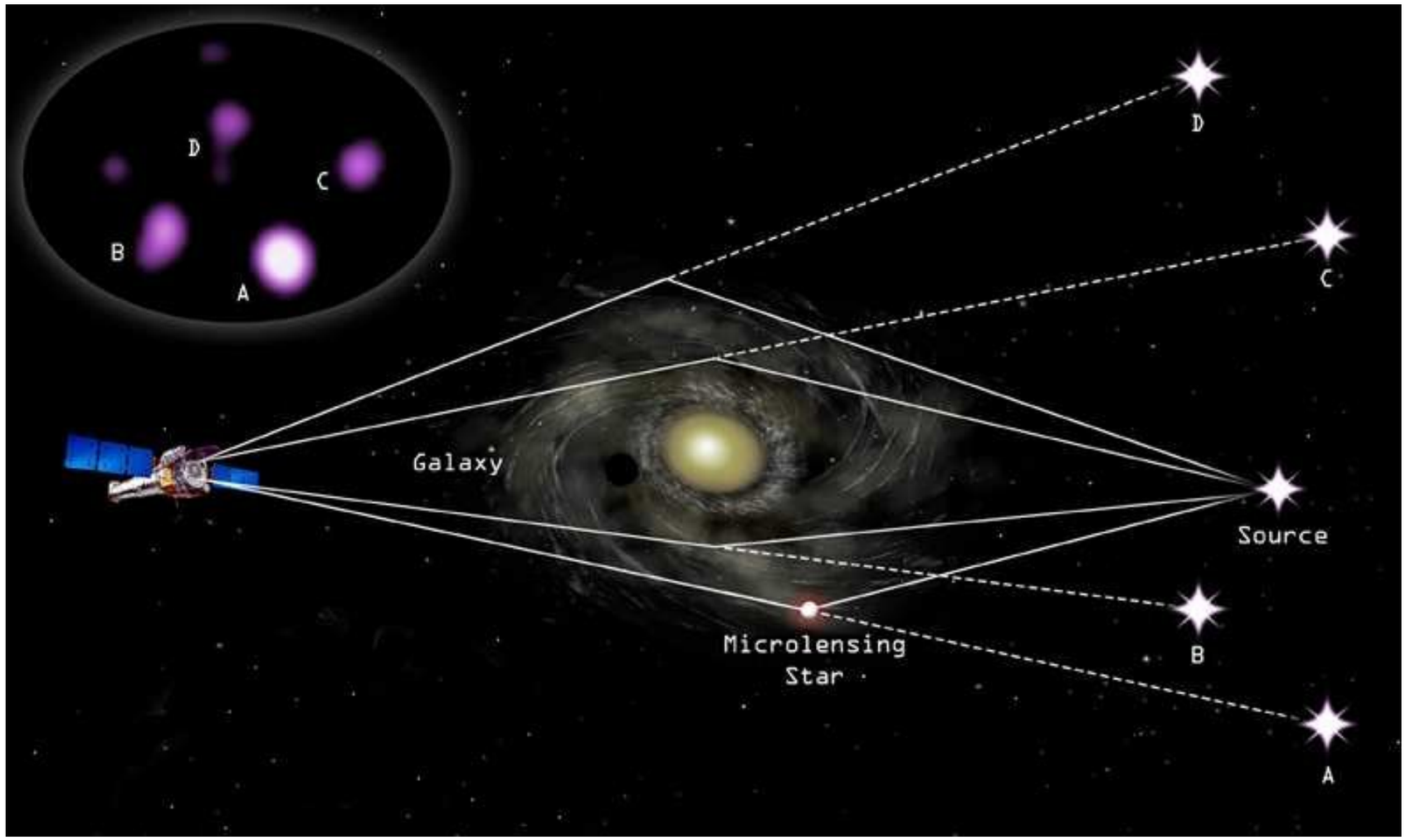

Anguita

Flux ratios of multiply-lensed quasars

Microlensing by compact objects in the lens galaxy leads to variations variation in the brightness of multiple-image quasars. Chang and Refsdal

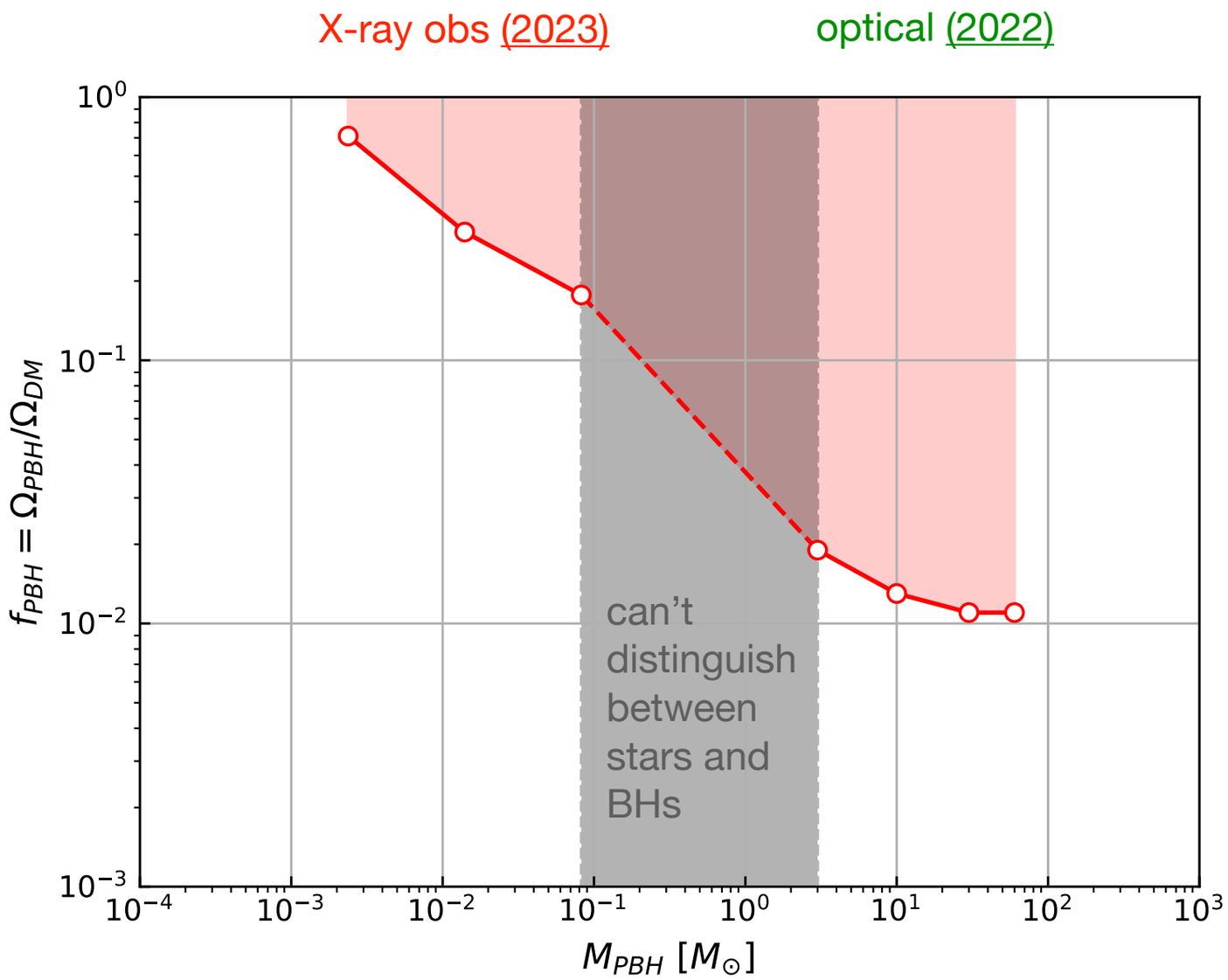

Esteban-Gutierrez et al. (2023)

Compilation of microlensing constraints

(under ‘standard’ assumptions, including a delta-function PBH mass function)

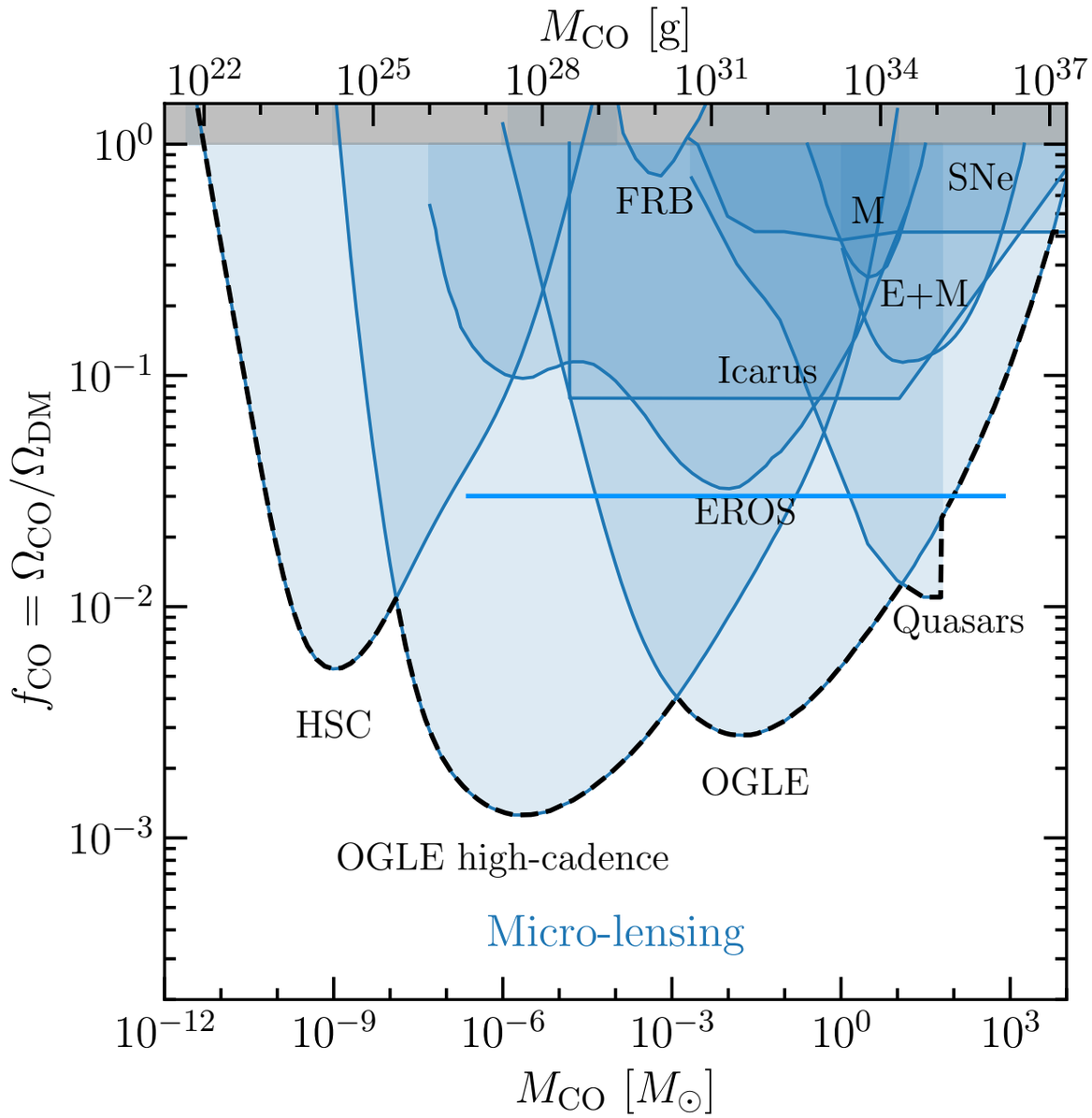

9 supermagnified stars

https://github.com/bradkav/PBHbounds

2. Effect of PBH distribution on LMC microlensing constraints

Reliability of constraints (or best-fit parameters) depends on reliability of assumptions and modelling.

Will focus in this talk on the density profile, $\rho(r)$, and velocity distribution, and assume PBHs are smoothly distributed.

Clusters formed from collapse of large gaussian density perturbations are sufficiently diffuse that PBHs lens individually, and in this case effect of clusters on microlensing constraints is very small Petaĉ, Lavalle & Jedamzik; Gorton & Green.

But

- non-gaussianity leads to larger clustering e.g. Young & Byrnes, Animali & Vennin
- if clusters are sufficiently compact, the cluster as a whole acts as a lens, and microlensing constraints shifted to smaller M Calcino, Garcia-Bellido & Davis

Differential event rate

assuming a delta-function lens mass function and a spherical halo with a Maxwellian velocity distribution: Griest

$$\frac{\mathrm{d}\Gamma}{\mathrm{d}\hat{t}} = \frac{32L}{M\hat{t}^4 v_\mathrm{c}^2} \int_0^1 \rho(x) R_\mathrm{E}^4(x) \exp\left[-\frac{4R_\mathrm{E}^2(x)}{\hat{t}^2 v_\mathrm{c}^2}\right] \mathrm{d}x$$

$\rho(x)$ = compact object density distribution along line of sight

$\hat{t}$ = Einstein diameter crossing time (as used by the MACHO collab., EROS & OGLE use Einstein radius crossing time)

v_c = local circular speed (usually taken to be 220 km/s, ~10% uncertainty)

Expected number of events:

$$N_\mathrm{exp} = E \int_0^\infty \frac{\mathrm{d}\Gamma}{\mathrm{d}\hat{t}}\, \epsilon(\hat{t})\, \mathrm{d}\hat{t}$$

E = exposure (number of stars times duration of obs.)

$\epsilon(\hat{t})$ = efficiency

For smoothly distributed DM the distribution of the number of events observed, N_obs, is Poissonian, so if $N_\mathrm{obs} = 0$, $N_\mathrm{exp} < 3$ at 95% confidence.

Standard halo model

cored isothermal sphere:

$$\rho(r) = \rho_0 \frac{R_c^2 + R_0^2}{R_c^2 + r^2}$$

$\rho_0 = 0.008\, M_\odot\, \mathrm{pc}^{-3}$, local dark matter density

$R_c = 5\,\mathrm{kpc}$, core radius

$R_0 = 8.5\,\mathrm{kpc}$, Solar radius

Evans' power law halo models Evans

'self-consistent' (velocity distribution consistent with halo density profile) & have analytic expressions for microlensing differential event rate.

$$\rho(r) = \frac{v_a^2 r_c^\beta}{4\pi G} \frac{(1-\beta^2)r^2 + 3r_c^2}{(r^2 + r_c^2)^{(\beta+4)/2}} \qquad r \gg r_c : \qquad \rho(r) \propto r^{-(2+\beta)}$$

PL B $\beta = -0.2$ (massive halo, rising rotation curve)
PL C $\beta = +0.2$ (light halo, falling rotation curve)

Uncertainty in differential event rate and hence constraints

MACHO collaboration first year results paper: Alcock et al. (1996)

theoretical differential event rate
(assuming $f_{\rm PBH} = 1,\ M = 1M_\odot$ & perfect detection efficiency)

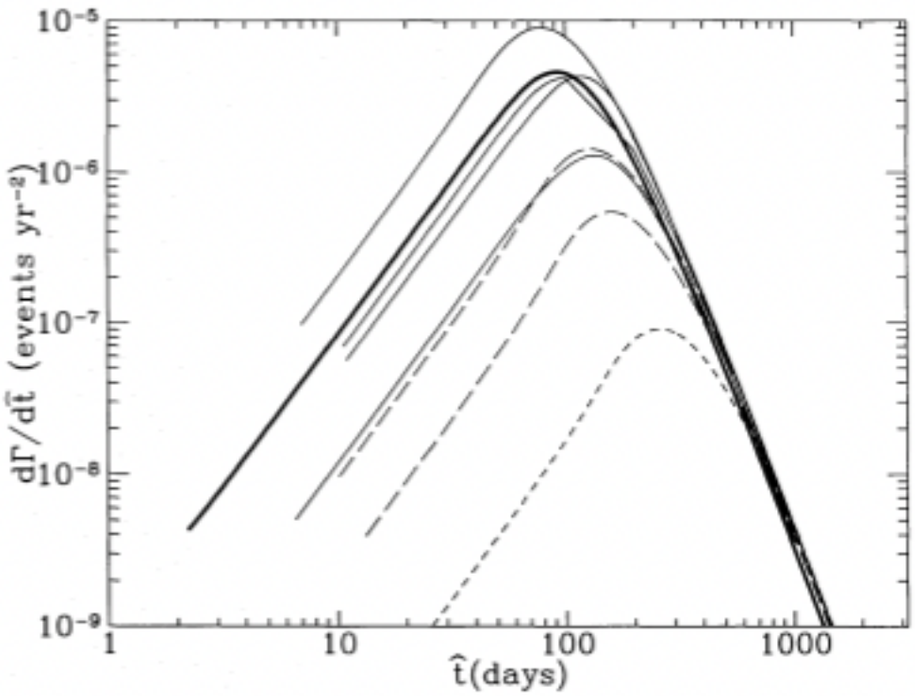

FIG. 11.—Theoretical differential event rates as a function of $\hat{t}$ for models described in Table 2. A delta function MACHO mass function at 1 $M_\odot$ is assumed; for other masses one simply scales the $\hat{t}$-axis by $\sqrt{m}$ and the rate-axis by m^{-1}, hence, the total event rate scales as $m^{-0.5}$. The thick solid line shows the standard model S, the thin solid lines show models B (highest), A, D, and C (lowest). The short-dashed line shows the maximal disk model E, and the long-dashed lines show the large disk models F and G.

MACHO 1 year
exclusion limit

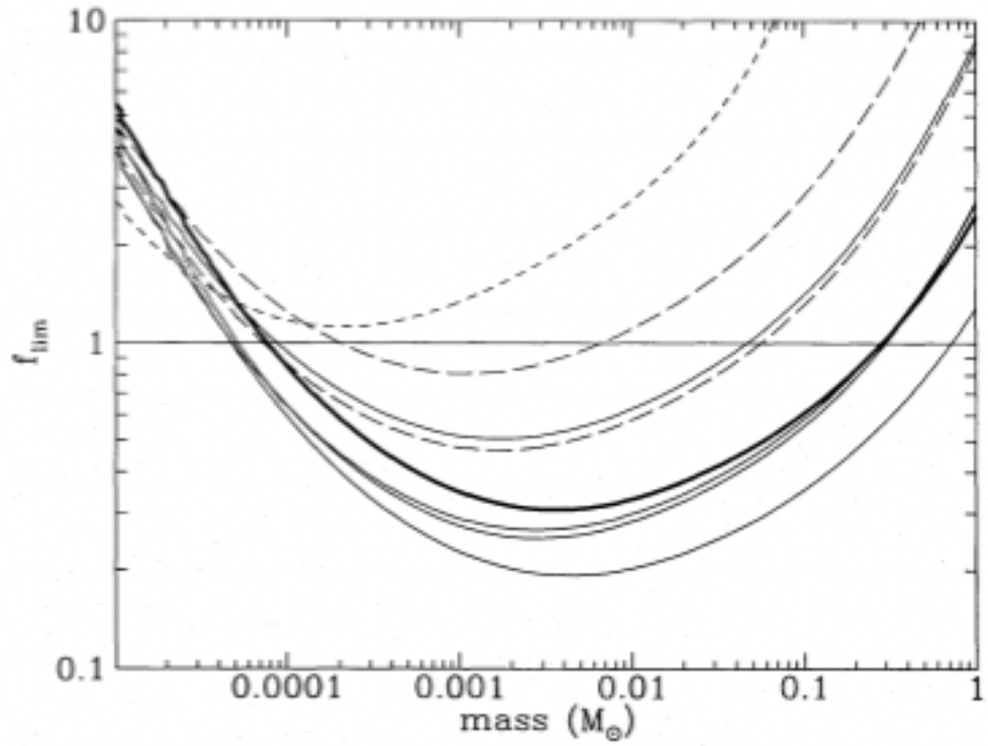

FIG. 13.—95% CL upper limits on the MACHO halo fraction as a function of the MACHO mass for the models described in Table 2. The lines are coded as in Fig. 11.

for other masses: $\hat{t} \propto M^{1/2} \qquad \dfrac{d\Gamma}{d\hat{t}} \propto M^{-1}$

Griest

theoretical differential event rate

$f_{\rm PBH} = 1,\ M = 1 M_\odot$

$$\frac{d\Gamma}{d\hat{t}}$$

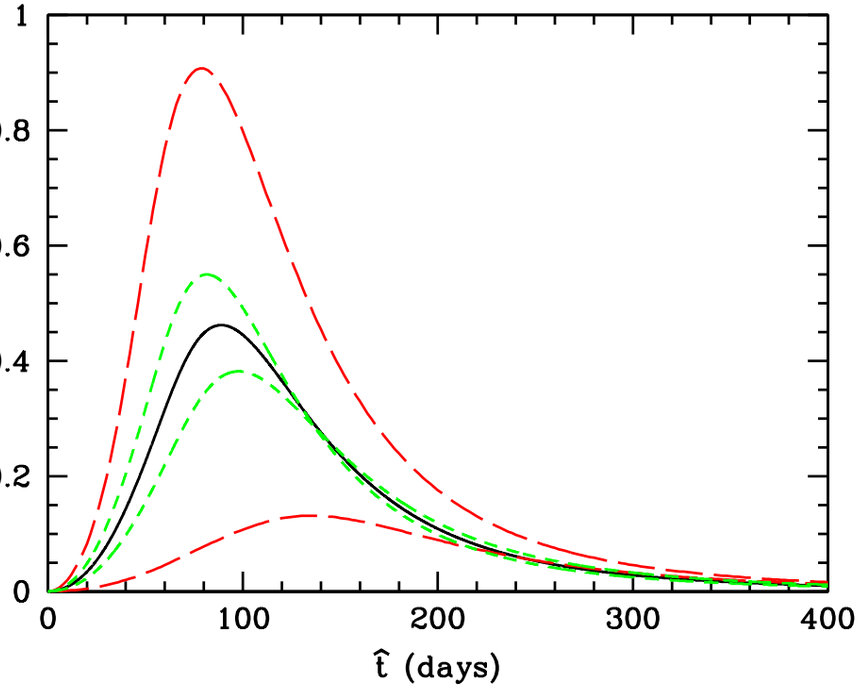

Einstein diameter crossing time (days)

EROS exclusion limit

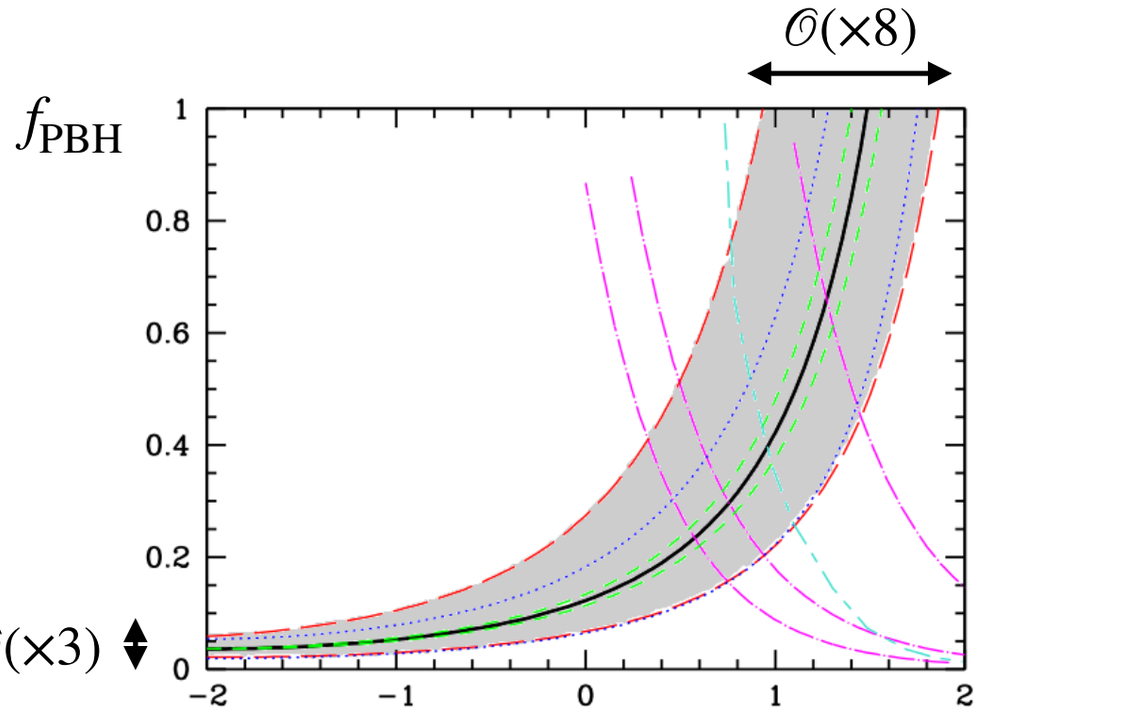

$\log_{10}(M/M_\odot)$

———— standard halo (SH), cored isothermal sphere, large r: $\rho \propto r^{-2}$, flat rotation curve

— — — power law halos B (massive halo, rising rotation curve) and C (light halo, falling rotation curve)

- - - - - SH local circular speed, 200 & 240 km/s

..... SH local density, 0.005 and 0.015

Green (2017)

see also Hawkins (2015)

Falling MW rotation curve from *Gaia* DR3?

Three different studies using *Gaia* DR3 data find a declining MW rotation curve:

$$v_{\rm c}^2(R) = R \left. \frac{\partial \Phi}{\partial R} \right|_{z \approx 0}$$

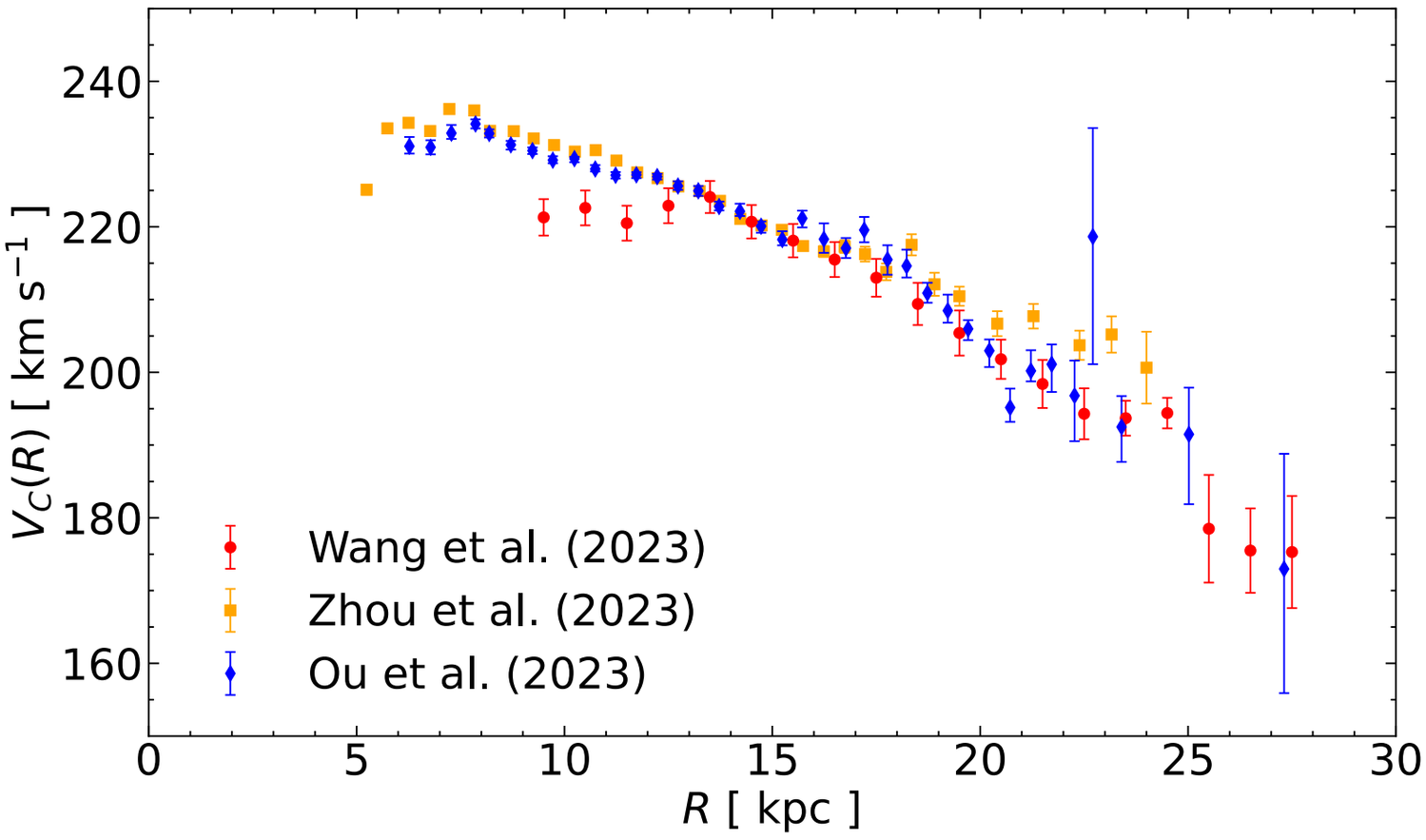

Jiao et al.

Caveats:

(Extrapolating to large R) gives significantly smaller MW halo mass ($0.2 \times 10^{12} M_\odot$) than from other probes (stellar streams, globular clusters, dwarf galaxies): $(0.7 - 1.1) \times 10^{12} M_\odot$.

~10% systematic uncertainties, in particular if density of tracer stars has a sharp truncation assuming exponential would lead to erroneous steeply declining rotation curve. Koop, Antoja, Helmi et al.

Garcia-Bellido & Hawkins (2024) find that MACHO . . . . and EROS - - - - limits change signifcantly:

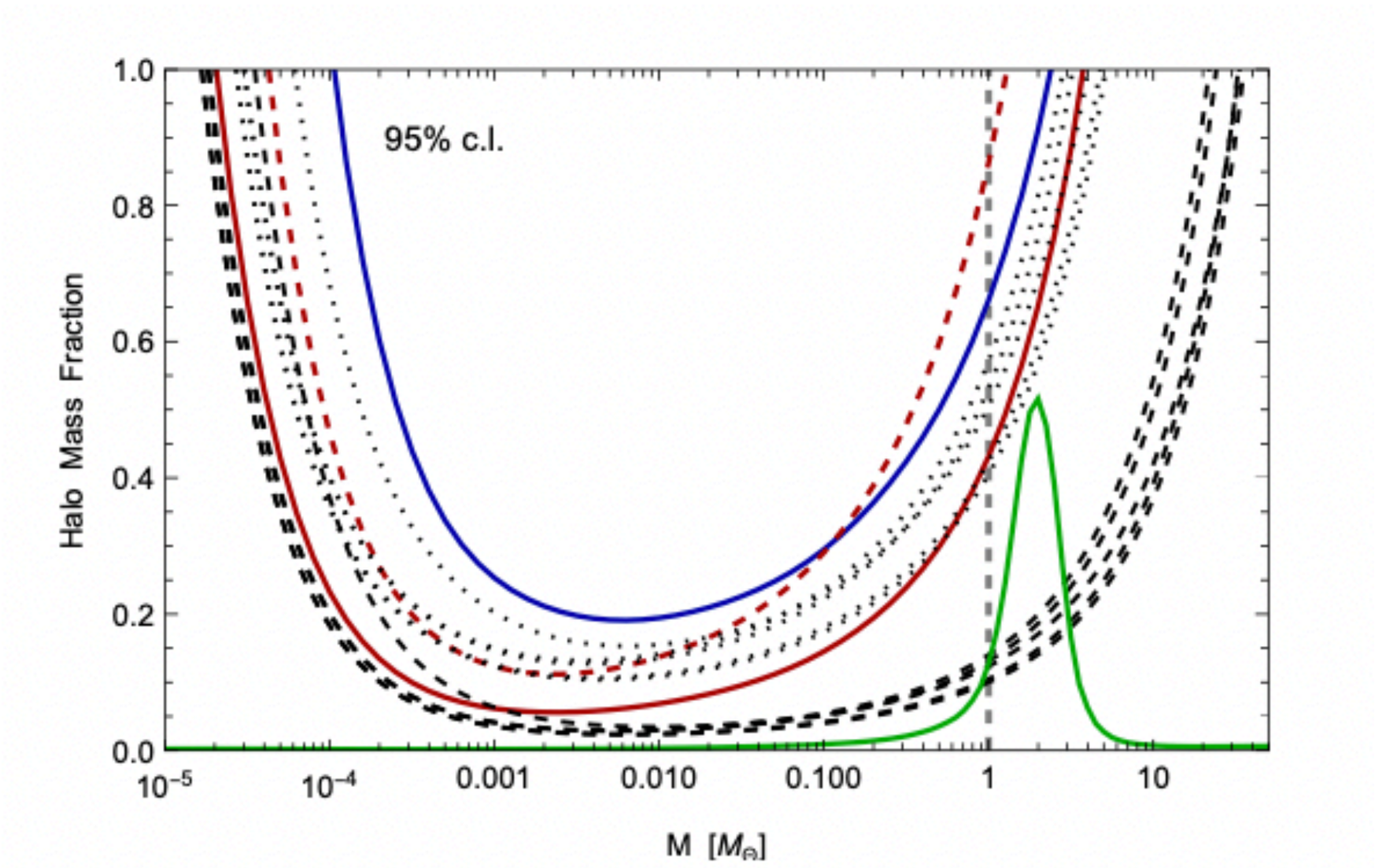

Fig. 5 The comparison between the old constraints (MACHO=dotted, EROS-2=dashed) and the new ones from MACHO (blue) and EROS-2 (red) at 95% c.l., with the dashed red curve corresponding to $N_{\rm obs} = 2$ in EROS. We also plot the Thermal History Model (green).

But Mroz et al. arXiv:2403.02386 find relatively small uncertainty/change in OGLE long exposure limit (assuming Maxwellian speed distribution):

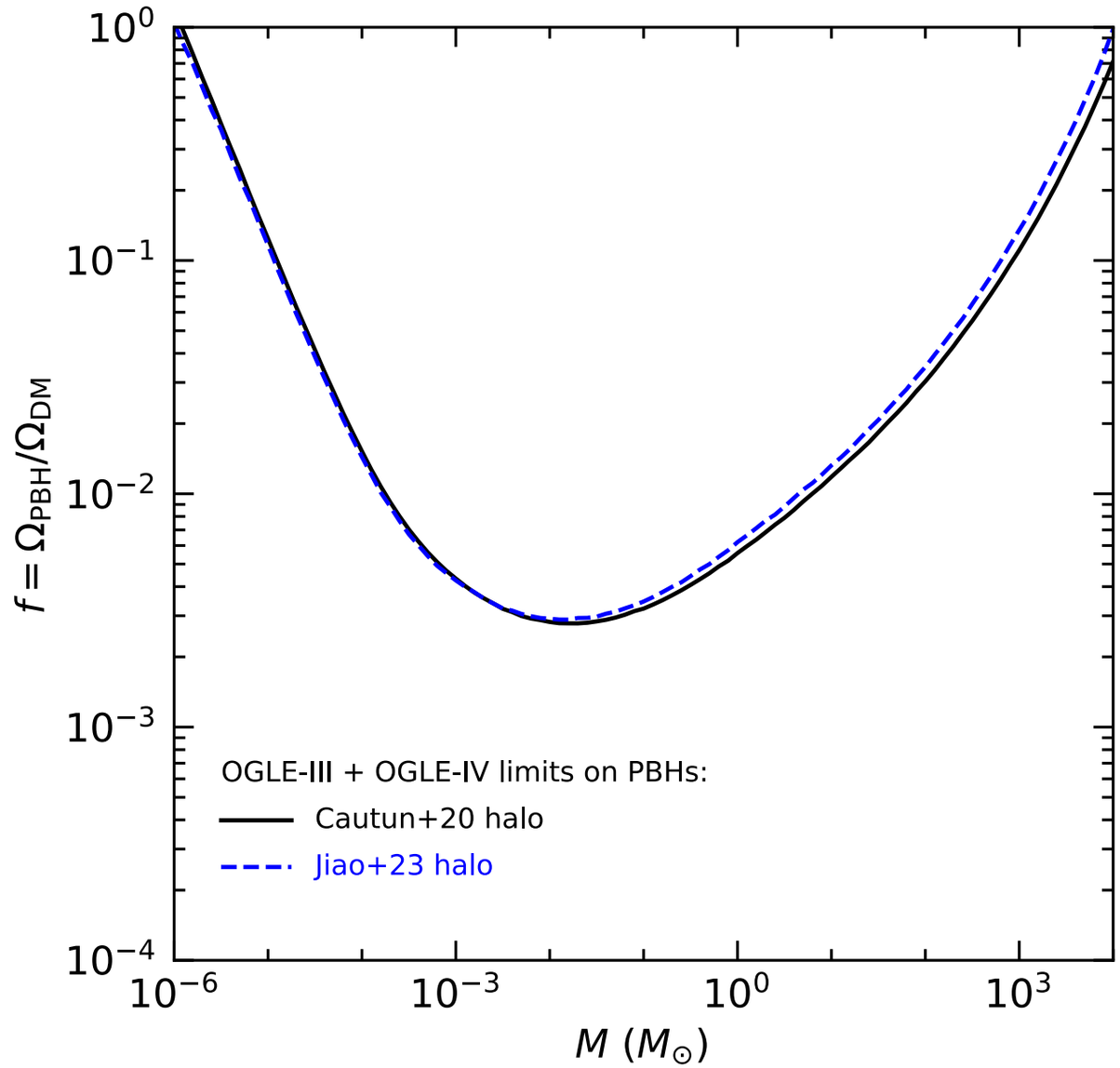

_____ Cautun et al. MW mass model fitted to *Gaia* DR2 rotation curve + other data., halo with contracted NFW profile (motivated by hydro simulations including baryons).

- - - - - - - - - Jiao et al. MW mass model fitted to declining *Gaia* DR3 rotation curve, halo with Einasto profile.

Towards understanding the uncertainty in the differential event rate

Work in progress!

short duration:

$\propto \hat{t}^2$

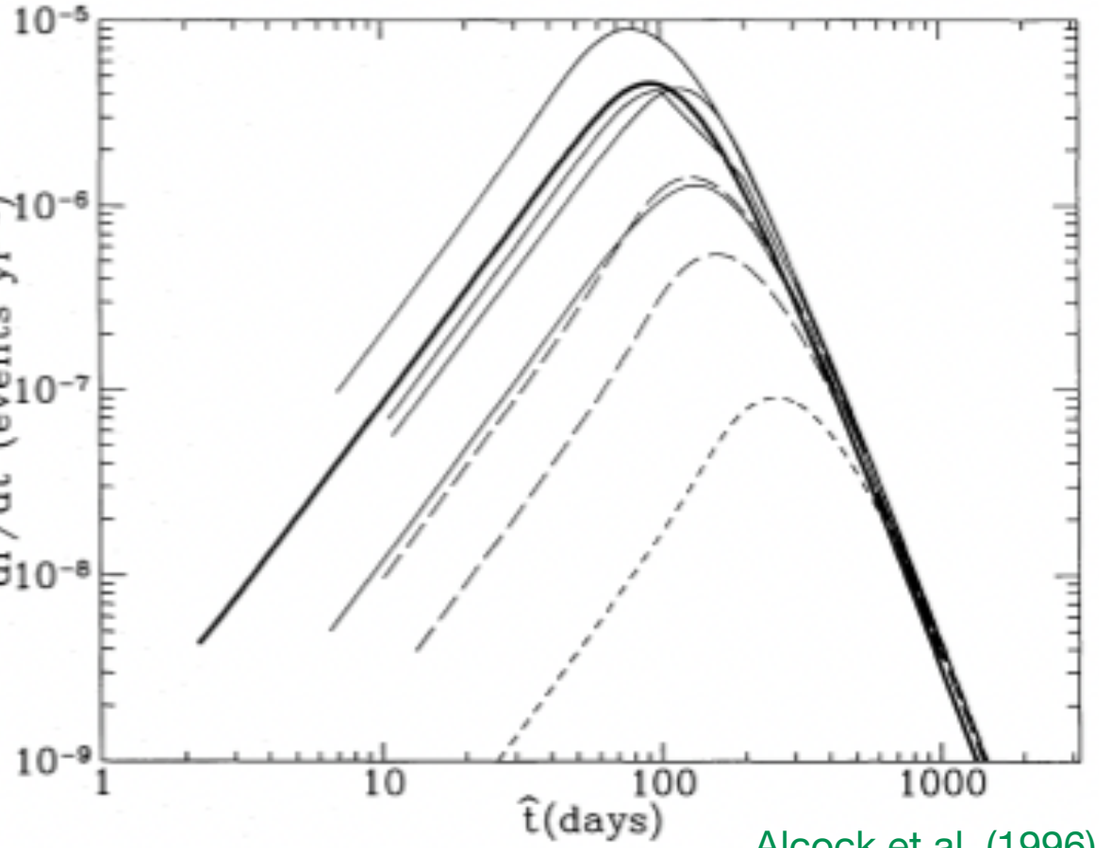

Alcock et al. (1996)

long duration:

$\propto \hat{t}^{-4}$

Mao & Paczynski (1996)

long duration events: lenses moving nearly along the line of sight, $\hat{t} \propto \sin^{-1} i \propto i^{-1}$

$$N \propto \frac{\Omega}{\hat{t}} \propto \frac{1-\cos\theta}{\hat{t}} \sim \frac{i^2}{i^{-1}} \sim i^3 \propto \hat{t}^{-3}$$

short duration events: lenses close to the observer ($x \sim 0$) or source, ($x \sim 1$)
for $x \sim 0$ (similar arguement holds for $x \sim 1$):

$$\hat{t} \propto r_{\rm E} \propto x\,, \qquad N \propto \frac{r_{\rm E} x}{\hat{t}} \propto \hat{t}^3$$

theoretical differential event rate

$$M = \left(10^{-6}, 10^{-3}, 1, 10^{3}\right) M_{\odot}$$

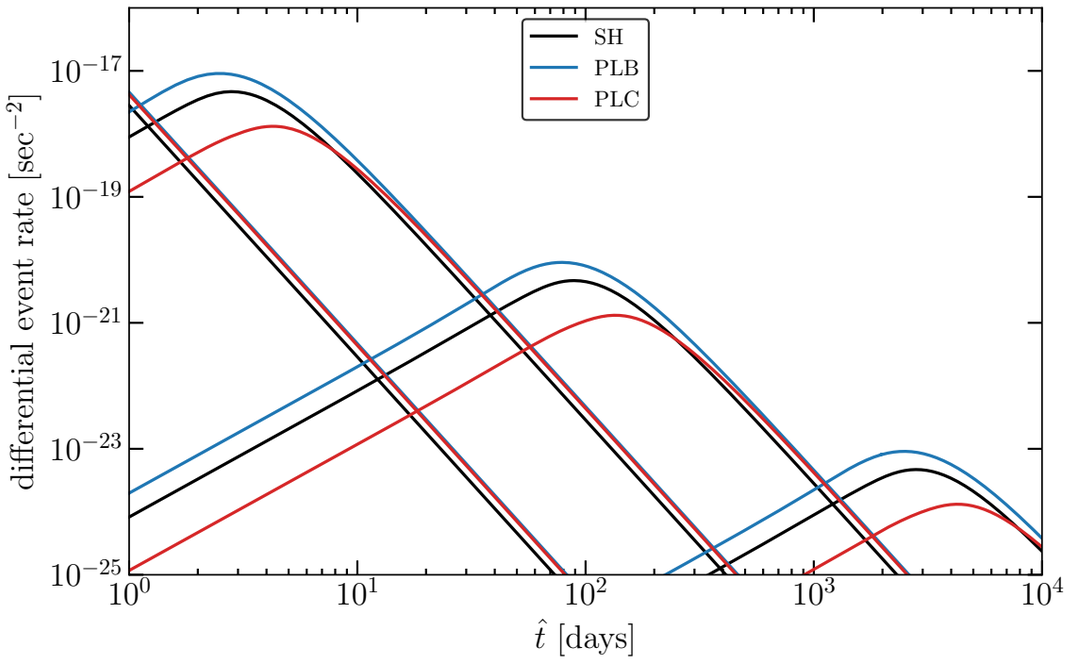

Constraints from a toy long exposure microlensing survey

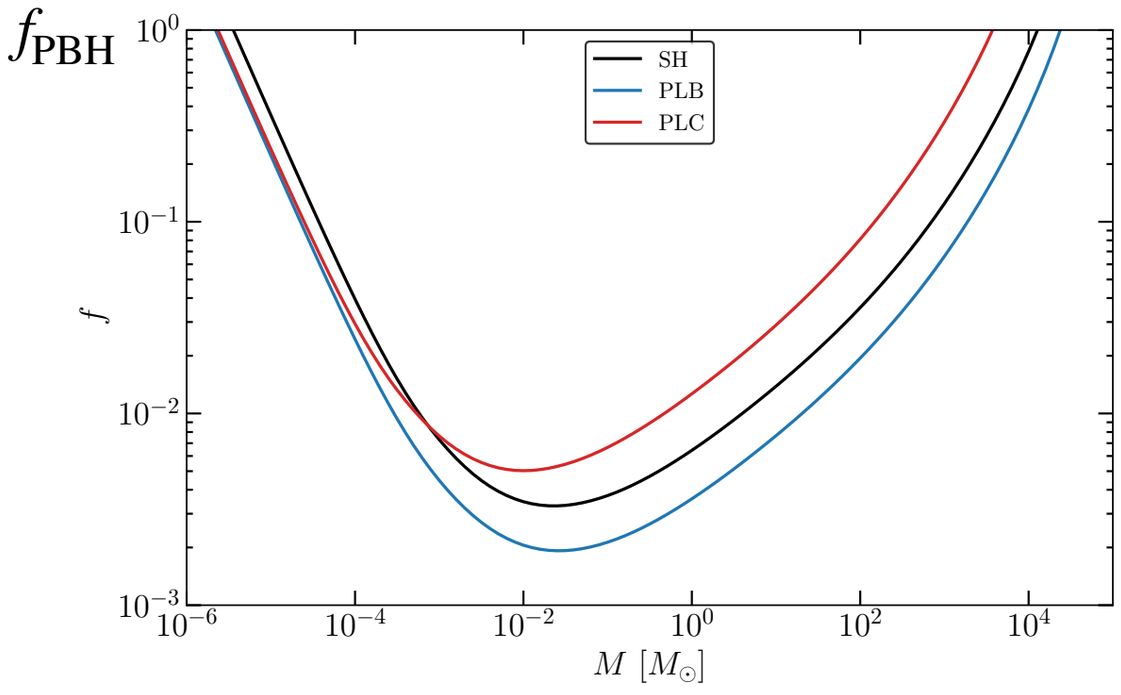

Light compact objects (COs): limit depends on long duration tail of differential event rate.

Massive COs: limit depends on (more variable) short duration tail of differential event rate.

$$\frac{\mathrm{d}\Gamma}{\mathrm{d}\hat{t}} = \frac{512 L^3 G^2 M \rho_0}{\hat{t}^4 {v_\mathrm{c}}^2 c^4} \int_0^1 \tilde{\rho}(x) x^2 (1-x)^2 \exp\left[-Q(x)\right] \mathrm{d}x$$

$$\rho(x) = \rho_0 \tilde{\rho}(x)$$

$$Q(x) = x(1-x)\left(\frac{t_\mathrm{ref}}{\hat{t}}\right)^2 \qquad t_\mathrm{ref} \equiv \frac{4}{v_\mathrm{c}}\left(\frac{GML}{c^2}\right)^{1/2} \sim 1\,\mathrm{yr}\left(\frac{M}{1 M_\odot}\right)^{1/2}$$

long duration events ($\hat{t} \gg t_\mathrm{ref}$)

$Q(x) \approx 0$ and $\exp[-Q(x)] \approx 1$ so

$$\frac{\mathrm{d}\Gamma}{\mathrm{d}\hat{t}} = \frac{512 L^3 G^2 M \rho_0}{\hat{t}^4 {v_\mathrm{c}}^2 c^4} \int_0^1 \tilde{\rho}(x) x^2 (1-x)^2 \mathrm{d}x$$

(neglecting the contribution of non-halo components of MW) $v_\mathrm{c}^2 \propto \rho_0$

Integrand independent of $\hat{t}$ (and M), largest for $x \approx 0.25$. Integral just depends on density of COs within microlensing tube.

Halo model dependence of amplitude of long-duration tail (& hence low M limits) is relatively small.

$$\frac{\mathrm{d}\Gamma}{\mathrm{d}\hat{t}} = \frac{512 L^3 G^2 M \rho_0}{\hat{t}^4 {v_\mathrm{c}}^2 c^4} \int_0^1 \tilde{\rho}(x) x^2 (1-x)^2 \exp\left[-Q(x)\right] \mathrm{d}x$$

$$\rho(x) = \rho_0 \tilde{\rho}(x)$$

$$Q(x) = x(1-x)\left(\frac{t_\mathrm{ref}}{\hat{t}}\right)^2 \qquad t_\mathrm{ref} \equiv \frac{4}{v_\mathrm{c}}\left(\frac{GML}{c^2}\right)^{1/2} \sim 1\,\mathrm{yr}\left(\frac{M}{1 M_\odot}\right)^{1/2}$$

short duration events ($\hat{t} \ll t_\mathrm{ref}$)

Unless $x \approx 0$ or $x \approx 1$, $Q(x)$ is large and $\exp[-Q(x)] \approx 0$.

Using $$\int_0^\infty y^2 \exp\left(-Cy\right) \mathrm{d}y = \frac{2}{C^3}$$

$$\frac{\mathrm{d}\Gamma}{\mathrm{d}\hat{t}} \approx \frac{\rho_0 v_\mathrm{c}^4 c^2 \hat{t}^2}{4M^2 G}\left(1 + \tilde{\rho}(1)\right) \approx \frac{\rho_0 v_\mathrm{c}^4 c^2 \hat{t}^2}{4M^2 G}$$

Depends on local density and typical speed of COs.

Halo model dependence of amplitude of short-duration tail (& hence high M limits) is not small.

Standard halo and power law halos with consistent $\rho_0/v_{\rm c}^2$ for $M = 1 M_\odot$

(if neglecting luminous components of MW, $v_{\rm c} \approx 177\,{\rm km\,s^{-1}}$, for SH for $\rho_0 = 0.008\,M_\odot {\rm pc}^{-3}$)

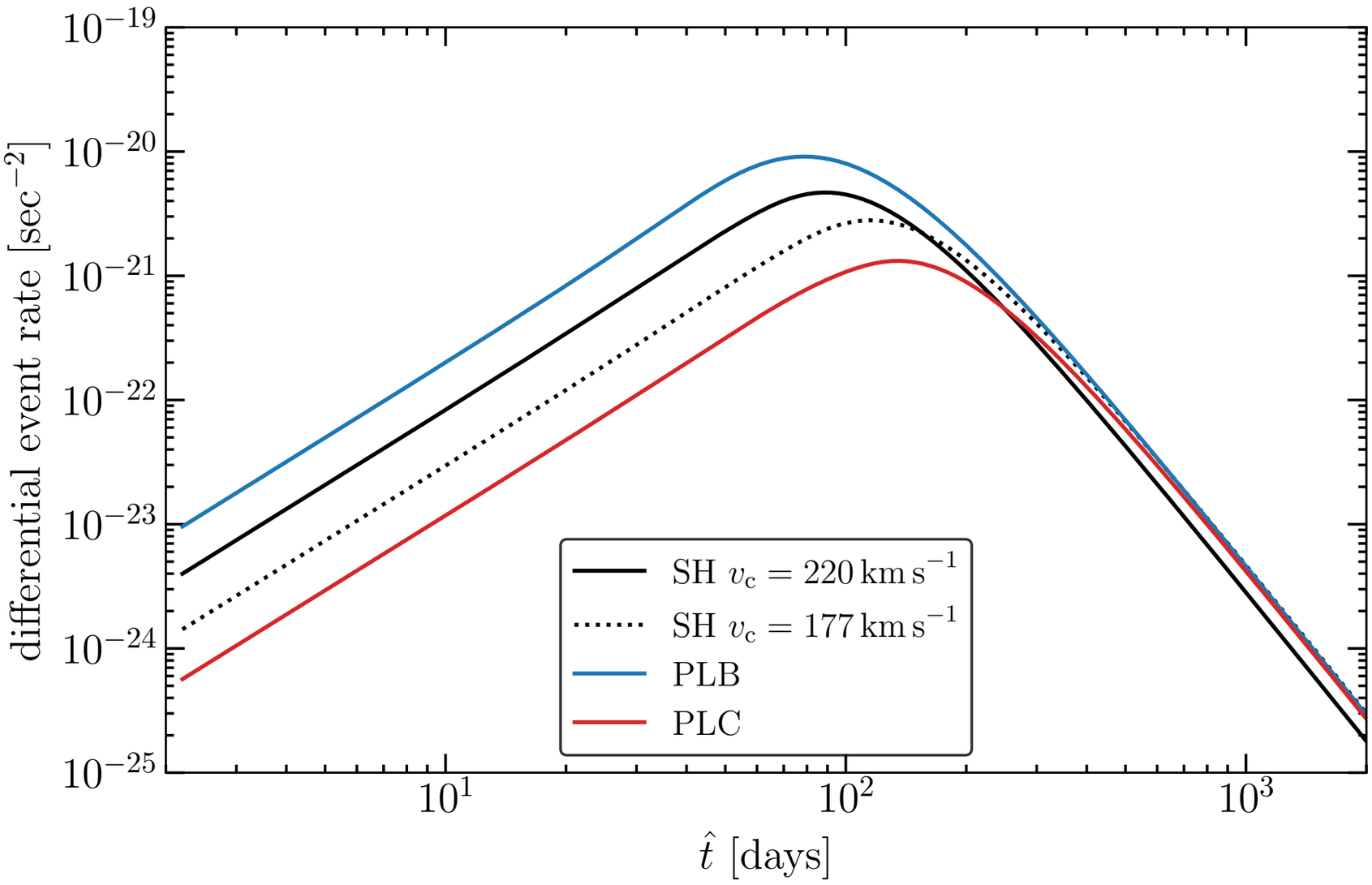

Effect of assuming gaussian $f(v)$ for PL halos?

relatively small, if v_c is chosen ‘appropriately’

Rotation curve: SH, PLB & PLC

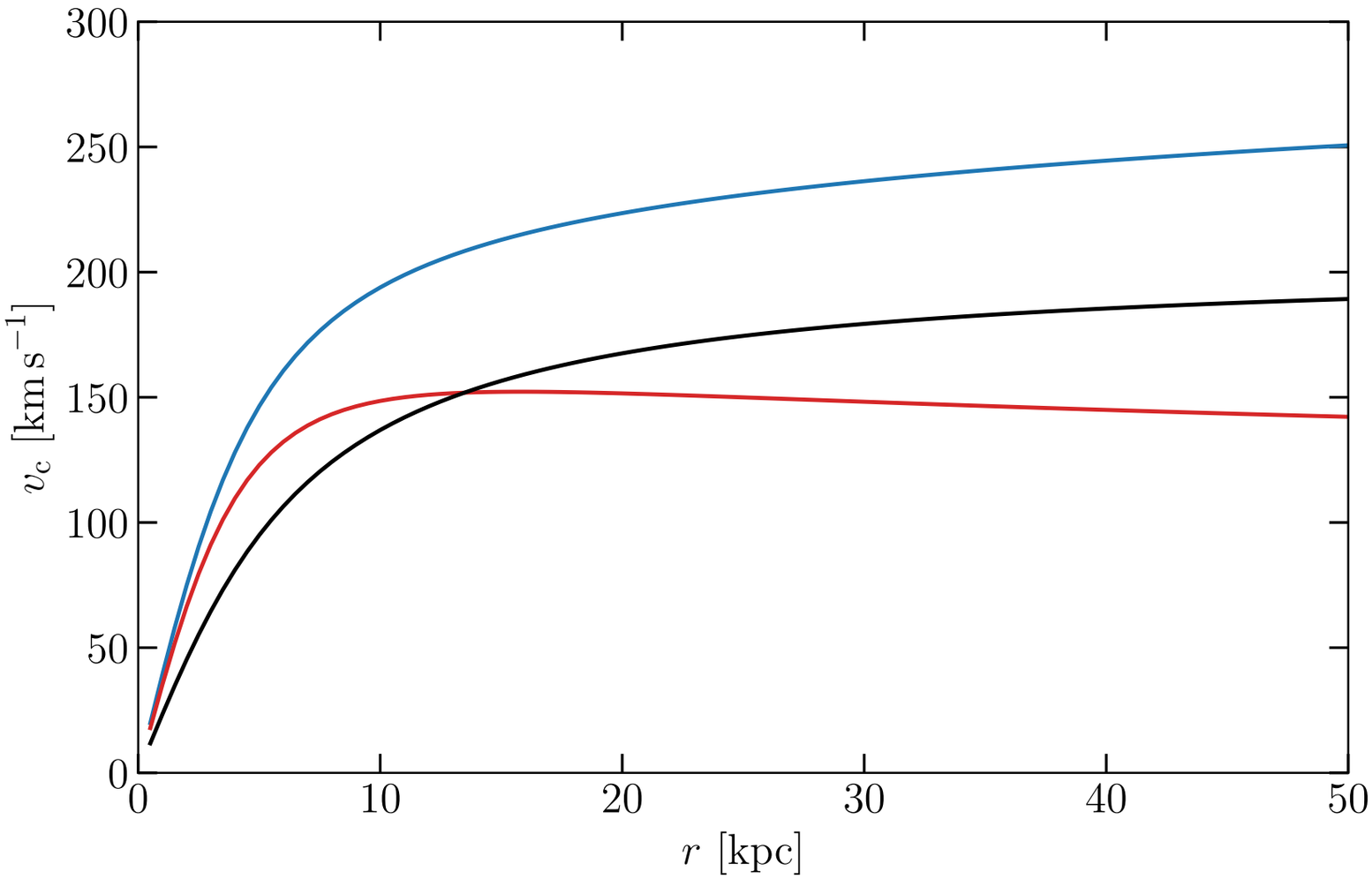

Effect of assuming gaussian $f(v)$ for PL halos?

relatively small, if v_c is chosen ‘appropriately’

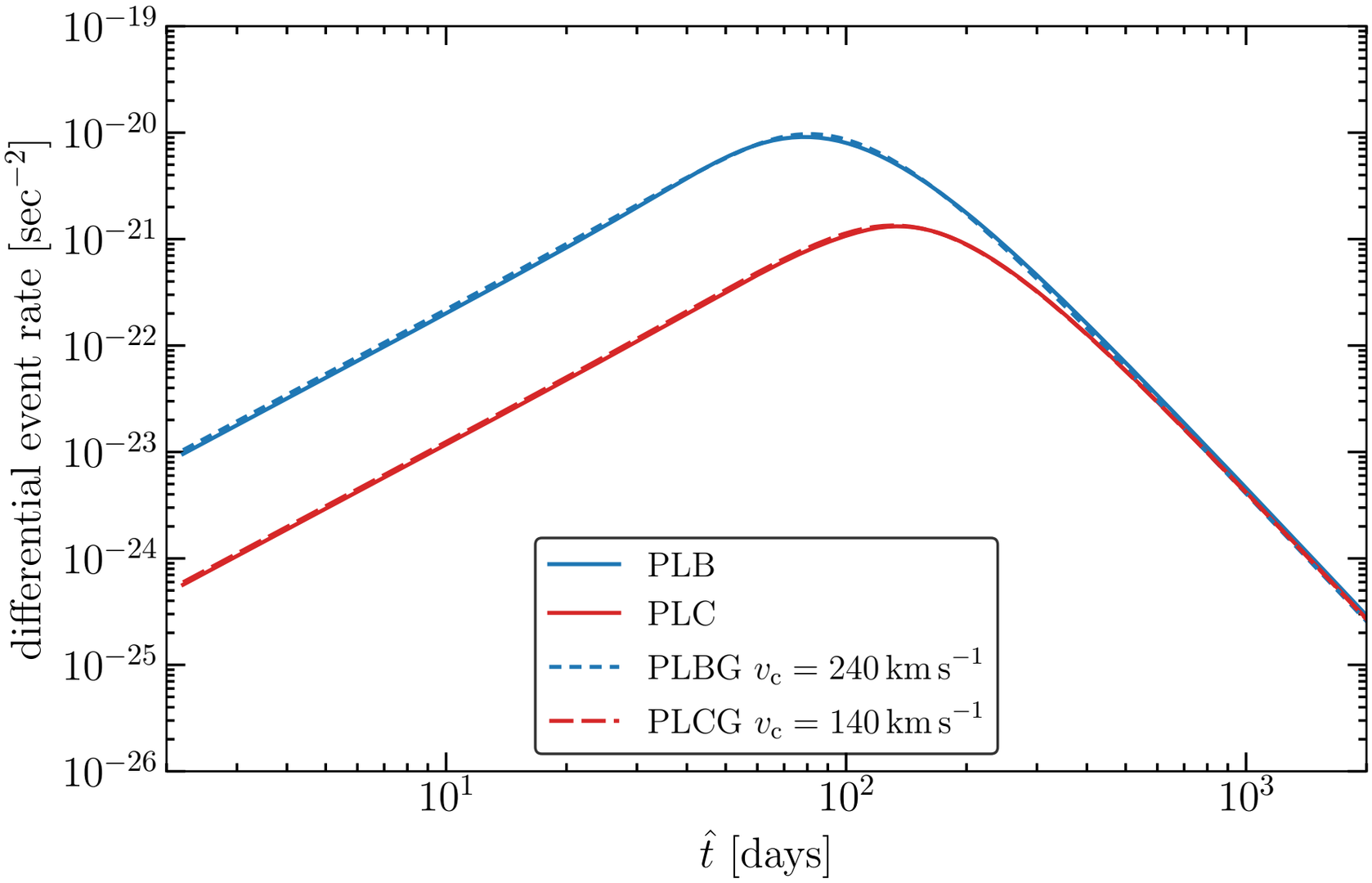

Summary

- Stellar microlensing observations (HSC, OGLE,…) place constraints:

$$f_{\rm PBH} \lesssim \mathcal{O}(10^{-2}) \text{ for } 10^{-10} M_\odot \lesssim M_{\rm PBH} \lesssim 10 M_\odot$$
$$f_{\rm PBH} \lesssim \mathcal{O}(1) \text{ for } 10^{-11} M_\odot \lesssim M_{\rm PBH} \lesssim 10^{4} M_\odot$$

  (under ‘standard’ assumptions about DM distribution).

- Several other microlensing observations (supermagnified stars, flux ratios of multiple lensed quasars) also constrain $f_{\rm PBH} \lesssim \mathcal{O}(10^{-1} - 10^{-2})$ for planetary and stellar mass PBHs.

- Uncertainties in stellar microlensing constraints from uncertainties in DM density profile (work in progress):

  small for long-duration tail of event rate, and hence ‘low mass’ constraints,

  larger for short-duration tail and hence ‘high mass’ constraints

Back-up slides

Compilation of observational constraints

(under ‘standard’ assumptions, including a delta-function PBH mass function)

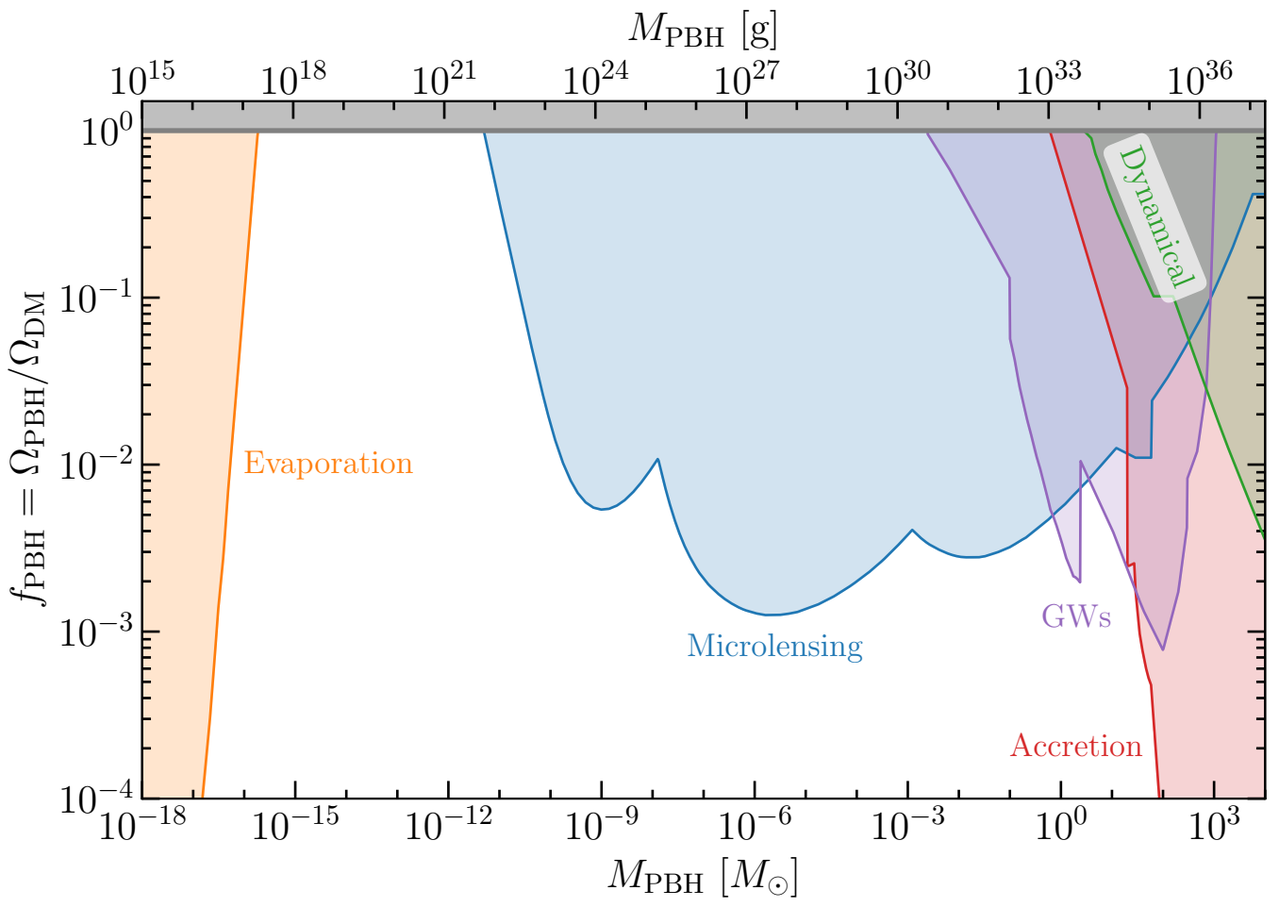

evaporation

lensing

gravitational waves

accretion

dynamical

https://github.com/bradkav/PBHbounds

Differential event rate for $M = 1\,M_\odot$ and halo fraction f=1:
($\hat{t} \propto M^{1/2}$, $\quad \mathrm{d}\Gamma/\mathrm{d}\hat{t} \propto M^{-1}$)

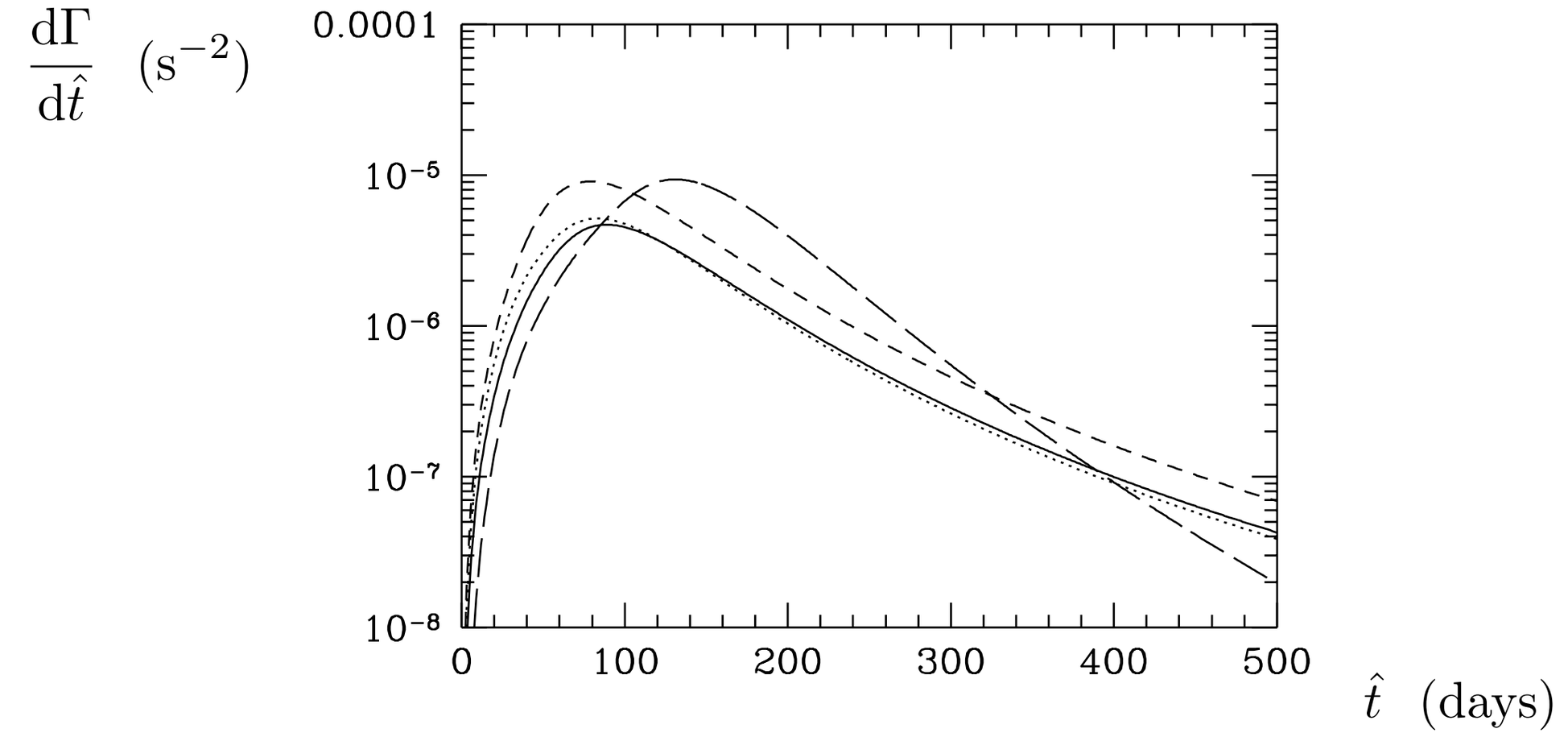

_____ = standard halo model

. . . . . = standard halo model including transverse velocity

- - - - = Evans power law model: massive halo with rising rotation curve, $v_\mathrm{c} \propto R^{0.2}$

_ _ _ _ = Evans power law model: flattened halo with falling rotation curve, $v_\mathrm{c} \propto R^{-0.2}$

velocity anisotropy can affect rate at ~10% level [De Paolis, Ingrosso & Jetzer]

Observations

MACHO

Monitored 12 million stars in LMC for 5.7 years.

Found 13/17 events (for selection criteria A/B, B less restrictive-picks-up exotic events).

Detection efficiency

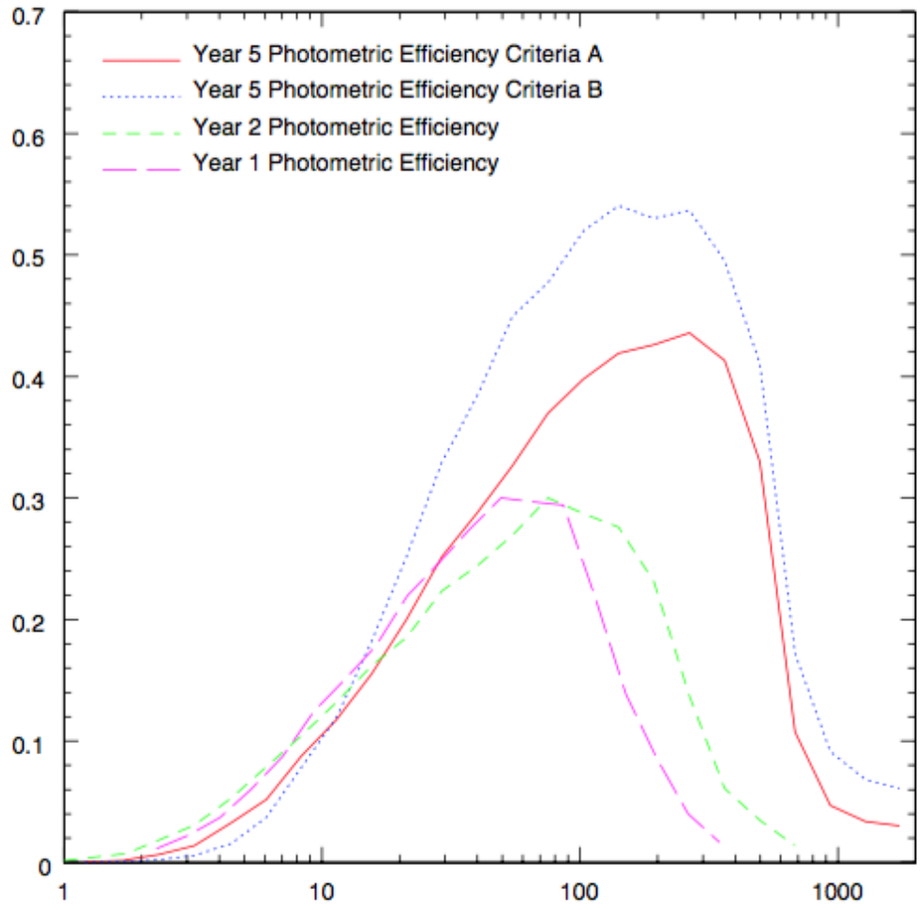

5 years A
5 years B
2 years
1 year

BUT

MACHO-LMC-5: lens identified (using HST obs & parallax fit) as a low mass MW disc star. [Drake et al.]

MACHO-LMC-7: OGLE-III light curve has multiple peaks, some sort of repeating outbursting variable star. [OGLE]

MACHO-LMC-9: (only satisfied criteria B) lens is a binary, allowing measurement of low projected velocity, which suggests lens is in LMC (or source is also binary). [MACHO]

MACHO-LMC-14: source is binary, and lens most likely to lie in LMC. [MACHO]

MACHO-LMC-20: (only B) lens identified (using Spitzer obs) as a MW thick disc star. [Kallivayalil et al.]

MACHO-LMC-22: (only B) supernova or an AGN in background galaxy. [MACHO]

MACHO-LMC-23: varied again twice, so not microlensing [EROS/OGLE]

MACHO-LMC-8, 18 & 27 (only B): have periodic variation in baseline (could still be microlensing, but don't expect this many microlensing events with variable baseline) [OGLE]

EROS

Monitored 67 million stars in LMC and SMC for 6.7 years.

Use bright stars in sparse fields (to avoid complications due to ‘blending’-contribution to baseline flux from unresolved neighbouring star).

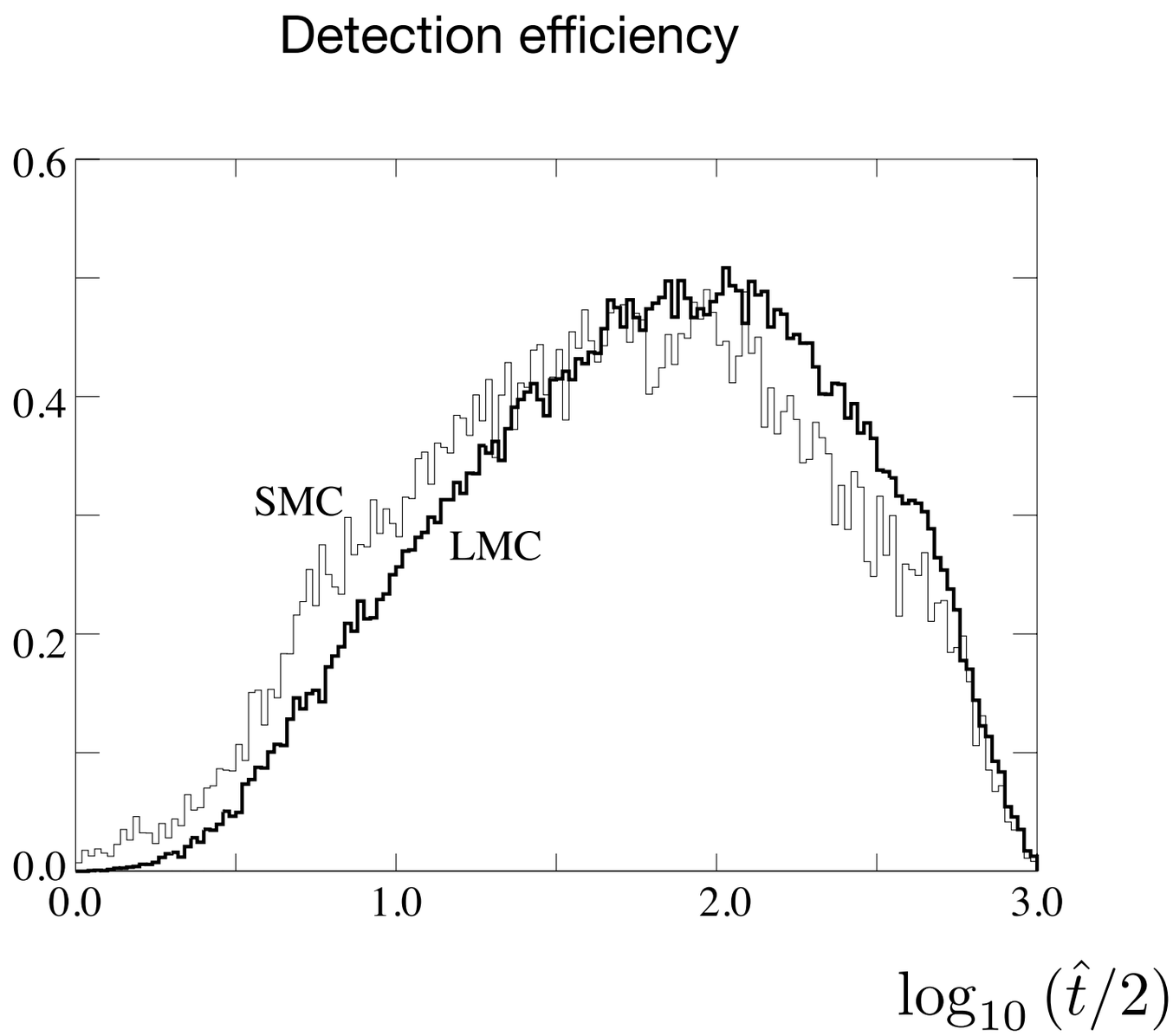

Final result: 1 SMC event (also seen by MACHO collab.) consistent (number & duration) with expectations for self-lensing (SMC is aligned along line of sight). [Graff & Gardiner]

Earlier candidate events eliminated: 7 varied again and 3 identified as supernovae.

Constraints on fraction of halo in compact objects, f,
(assuming a delta-function mass function):

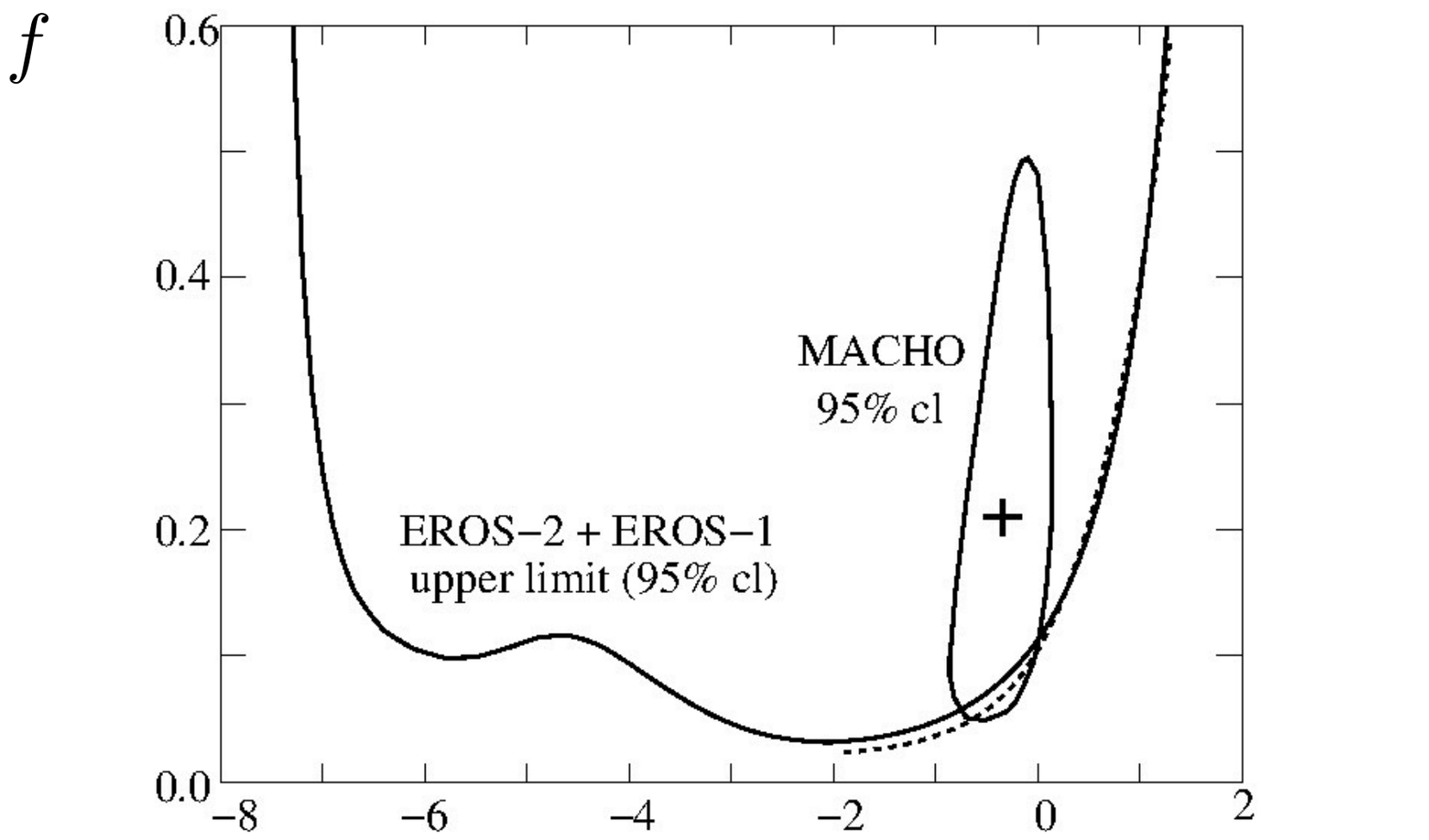

EROS

Phase space distribution function: $f(\mathbf{x}, \mathbf{v}, t)$

Number of particles with phase space co-ordinates in $\mathbf{x} \rightarrow \mathbf{x} + \mathrm{d}\mathbf{x}$ and $\mathbf{v} \rightarrow \mathbf{v} + \mathrm{d}\mathbf{v}$ at time t: $f(\mathbf{x}, \mathbf{v}, t)\mathrm{d}^3\mathbf{x}\mathrm{d}^3\mathbf{v}$

Steady-state phase space distribution of a collection of collisionless particles is given by the solution of the collisionless Boltzmann equation:

$$\frac{\mathrm{d}f}{\mathrm{d}t} = 0$$

in Cartesian co-ordinates:

$$\frac{\partial f}{\partial t} + \mathbf{v}.\frac{\partial f}{\partial \mathbf{x}} + \frac{\partial \Phi}{\partial \mathbf{x}}.\frac{\partial f}{\partial \mathbf{v}} = 0$$

Poisson's equation for a self-consistent system (where density distribution generates potential):

$$\nabla^2\Phi = 4\pi G\rho = 4\pi G \int f \mathrm{d}^3\mathbf{v}$$

A solution is:

$$\rho(r) = \frac{\sigma^2}{2\pi G r^2} \qquad f \propto \exp(-v^2/2\sigma^2)$$

c.f. the phase-space distribution of a self-gravitating isothermal sphere with

$$\sigma^2 = k_\mathrm{B}T/m$$

Collisionless particles can change their energy & reach the steady-state configuration if they experience a fluctuating gravitational potential (violent relaxation). However real DM halos haven't reached a steady state and contain substructure (subhalos and streams).

Analysis uses Jean's equations (found from taking velocity moments of collisionless Boltzmann equation), assumes MW is axisymmetric and in a steady state.

Also need to model density distribution of the tracer stars.

On the Galactic rotation curve inferred from the Jeans equations

Assessing its robustness using *Gaia* DR3 and cosmological simulations

Orlin Koop[1,⋆], Teresa Antoja[2], Amina Helmi[1], Thomas M. Callingham[1], and Chervin F. P. Laporte[2]

https://arxiv.org/abs/2405.19028

typical of galaxies that have been perturbed by external satellites. Also from the simulations we estimate that the difference between the true circular velocity curve and that inferred from Jeans equations can be as high as 15%, but that it likely is of order 10% for the Milky Way. This is of larger amplitude than the systematics associated to the observational uncertainties or those from most modelling assumptions when using the Jeans equations. However, if the density of the tracer population were truncated at large radii instead of being exponential as often assumed, this could lead to the erroneous conclusion of a steeply declining rotation curve.
Conclusions. We find that steady-state axisymmetric Jeans modelling becomes less robust at large radii, indicating that particular caution is needed when interpreting the rotation curve inferred in those regions. A more careful and sophisticated approach may be necessary for precision measurements of the dark matter content of our Galaxy.

Local circular speed e.g:

Reid et al. proper motion of Sgr A*:

$$v_c(R_\odot)/R_\odot = (30.3 \pm 0.9)\,\mathrm{km\,s^{-1}\,kpc^{-1}}$$

and using new precise measurement of $R_\odot$ gives

$$v_c(R_\odot) = (248 \pm 7)\,\mathrm{km\,s^{-1}\,kpc^{-1}}$$

Eilers et al. Jeans analysis from taking moment of collision less Boltzmann equations (in cylindrical co-ordinates):

$$v_c^2(R) = R\frac{\partial \Phi}{\partial R}_{z\approx 0} = \langle v_\phi^2 \rangle - \langle v_R^2 \rangle \left(1 + \frac{\partial \ln \nu}{\partial \ln R} + \frac{\partial \ln \langle v_R^2 \rangle}{\partial \ln R}\right)$$

ν = density of tracer stars.

combing data from Gaia, APOGEE and other sources:

$$v_c(R_\odot) = (229.0 \pm 0.2)\,\mathrm{km\,s^{-1}}$$

with (2-5)% systematic uncertainty (from e.g. uncertainty in distribution of tracer stars).

n.b. Standard halo has one-to-one relationship between circular speed and velocity dispersion & peak speed, but in general this isn't the case.

LMC microlensing constraints: clusters

Due to Poisson fluctuations in PBH distribution, PBH clusters form shortly after matter-radiation equality. Afshordi, Macdonald & Spergel; Inman & Ali-Haïmoud; Jedamzik

distribution at $z = 99$

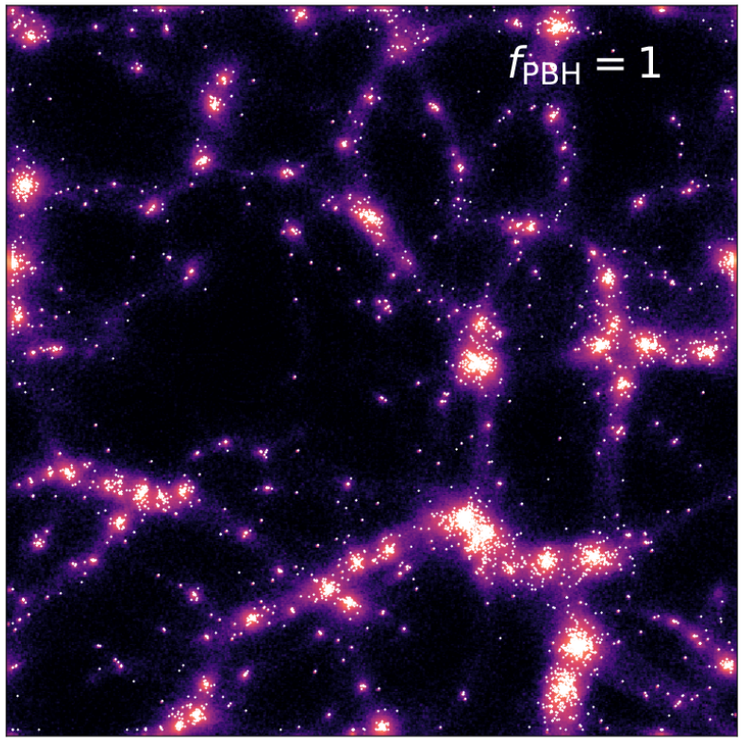

Inman & Ali-Haïmoud

Clusters containing a small number of PBHs, $N_{\rm cl}$, are most common, but those with $N_{\rm cl} \lesssim 10^3$ will evaporate by present day.

Clusters formed from gaussian perturbations are sufficiently extended that PBHs act as lenses indvidually (rather than the cluster as a whole). Petaĉ, Lavalle & Jedamzik; Gorton & Green

Clustering of PBHs formed from collapse of large density perturbations

PBHs don't form in clusters Ali-Haïmoud (previous work Chisholm extrapolated an expression for the correlation function beyond its range of validity).

However there are additional isocurvature perturbations (due to Poisson fluctuations in PBH distribution) and PBH clusters form shortly after matter-radiation equality.
Afshordi, Macdonald & Spergel; Inman & Ali-Haïmoud; Jedamzik

power spectrum

$P(k)$

$(\propto k^{n_s})$

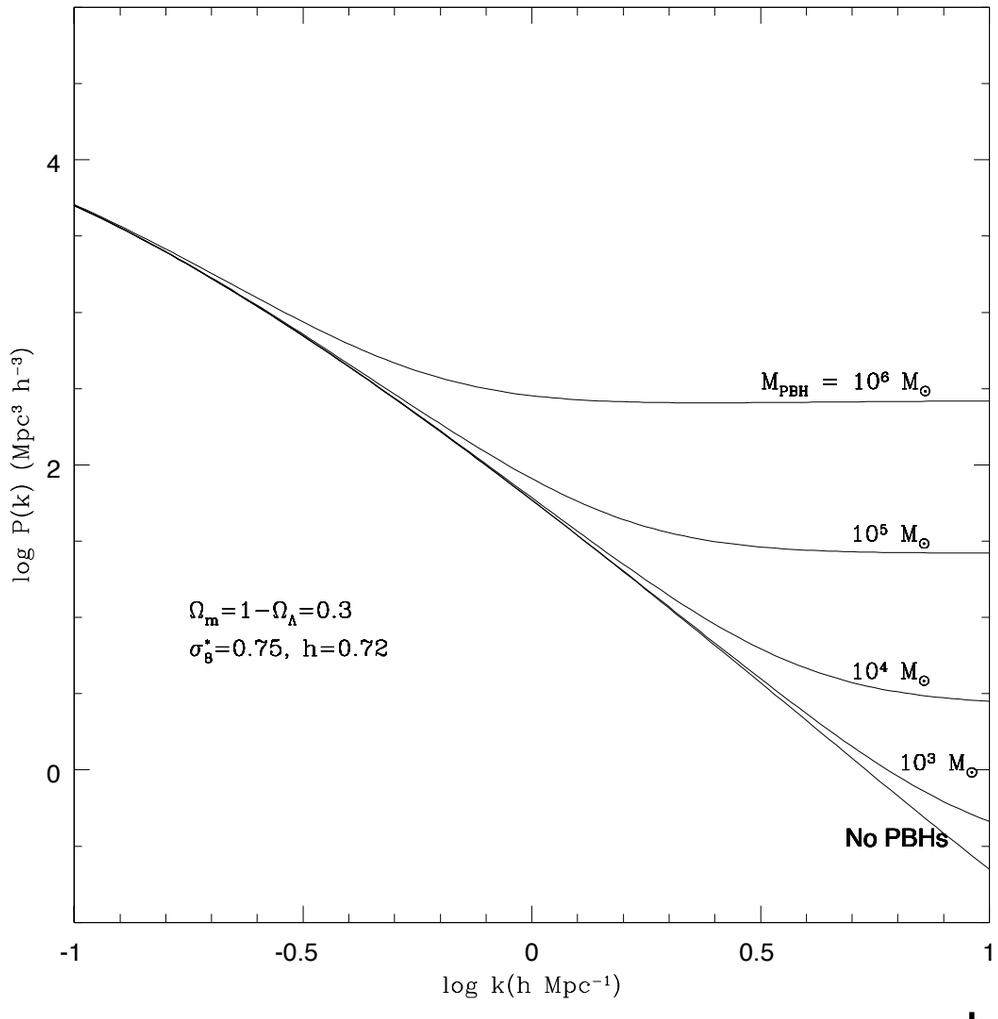

increasing PBH mass

no PBHs

k = comoving wavenumber

Afshordi, Macdonald & Spergel

Clustering of PBHs formed from collapse of large density perturbations

PBHs don't form in clusters Ali-Haïmoud (previous work Chisholm extrapolated an expression for the correlation function beyond its range of validity).

However there are additional isocurvature perturbations (due to Poisson fluctuations in PBH distribution) and PBH clusters form shortly after matter-radiation equality.
Afshordi, Macdonald & Spergel; Inman & Ali-Haïmoud; Jedamzik

mass variance

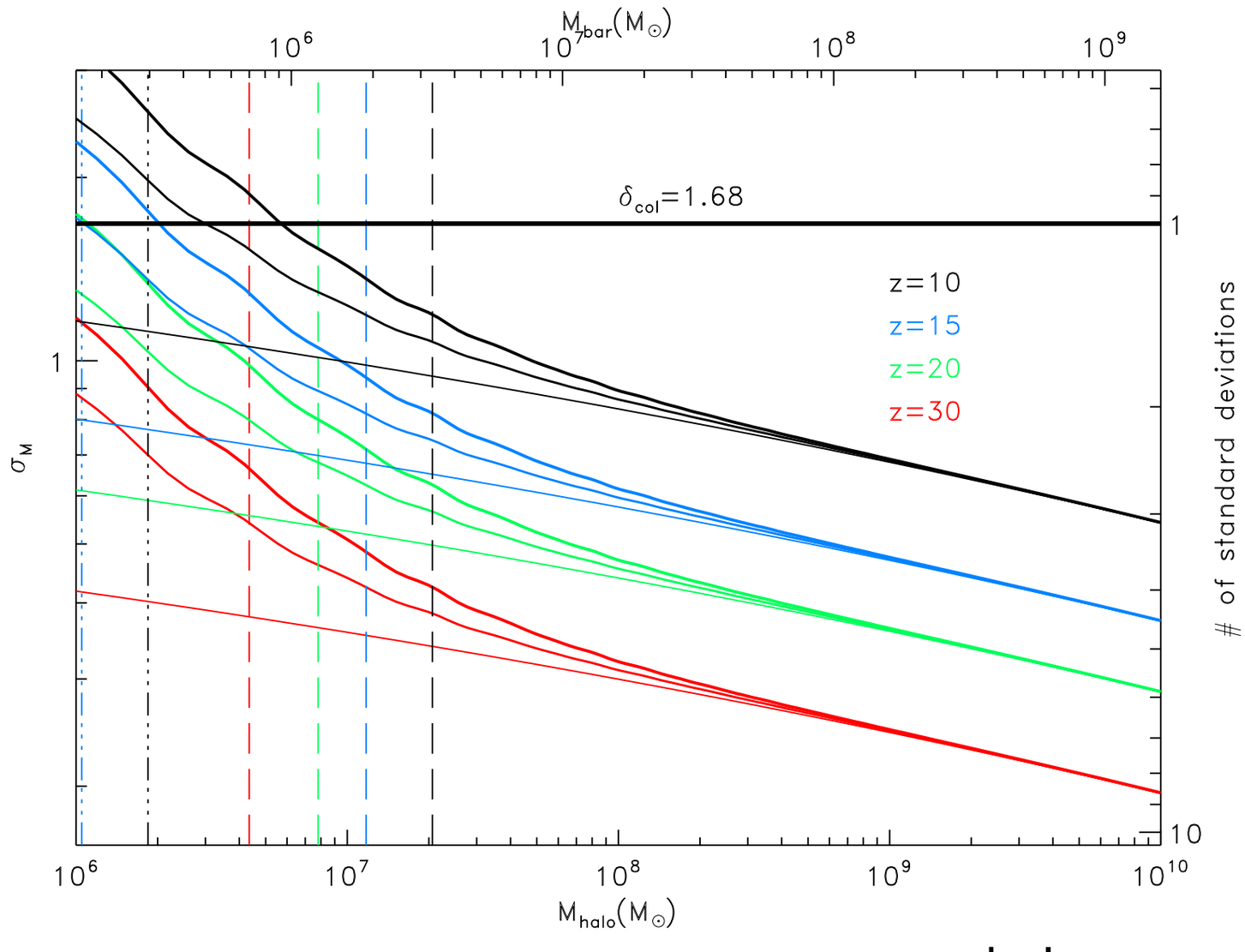

halo mass

Kashlinksy

← threshold for collapse

z= 10, 15, 20, 30

M_{PBH}=30 $M_\odot$

M_{PBH}=15 $M_\odot$

no PBHs

Approximate analytic calculation

c.f. Afshordi, Macdonald & Spergel; Jedamzik

PBH DM has additional isocurvature perturbations due to Poisson fluctuations in their distribution:

$$\delta(N) = \frac{\Delta N}{N} = \frac{1}{\sqrt{N}}$$

growth factor for isocurvature perturbations:

$$D(a) \approx \left(1 + \frac{3}{2}\frac{a}{a_{\rm eq}}\right)$$

spherical top hat collapse:

collapse occurs when:

$$D(a_{\rm col})\delta(N) = \delta_{\rm critical} \approx 1.69$$

final halo/cluster density:

$$\rho_{\rm cl} \approx 178\rho_{\rm DM}(a_{\rm coll})$$

radius of cluster:

$$r_{\rm cl} \approx 0.01\left(\frac{M_{\rm PBH}}{M_\odot}\right)^{1/3} N^{5/6}\,{\rm pc}$$

For $M_{\rm PBH} = M_\odot$, N=10 (100) clusters form at $z_{\rm coll}$ ≈1200 (320) and have $r_{\rm cl}$≈ 0.06 (0.5) pc.

N-body simulations

Inman & Ali-Haïmoud

Simulate a L = 30 h^{-1} kpc box, with $M_{\rm PBH} = 20 h^{-1} M_\odot$ from radiation domination to z = 99, for $f_{\rm PBH} = 1$ and also $f_{\rm PBH} < 1$ + particle dark matter.

matter field at z=100

$f_{\rm PBH} = 10^{-5}$

a PBH!

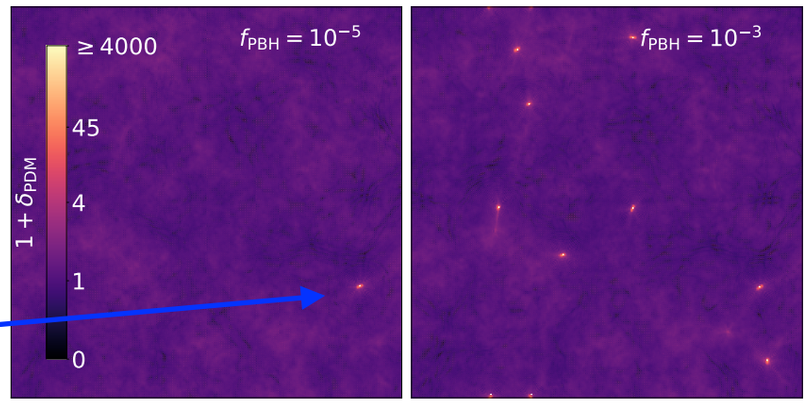

$f_{\rm PBH} = 10^{-3}$

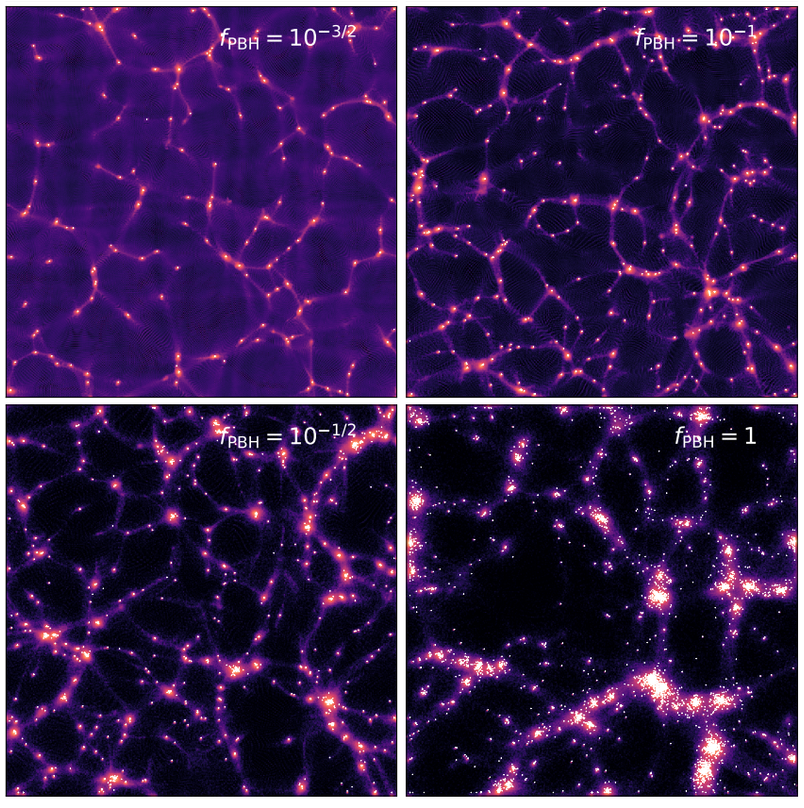

$f_{\rm PBH} = 10^{-3/2}$

$f_{\rm PBH} = 10^{-1}$

$f_{\rm PBH} = 10^{-1/2}$

$f_{\rm PBH} = 1$

Inman & Ali-Haïmoud

Clusters containing small numbers of PBHs always most abundant, but abundance of clusters containing large numbers of PBHs increases with time.

halo mass function (number of halos containing a given number of PBHs)

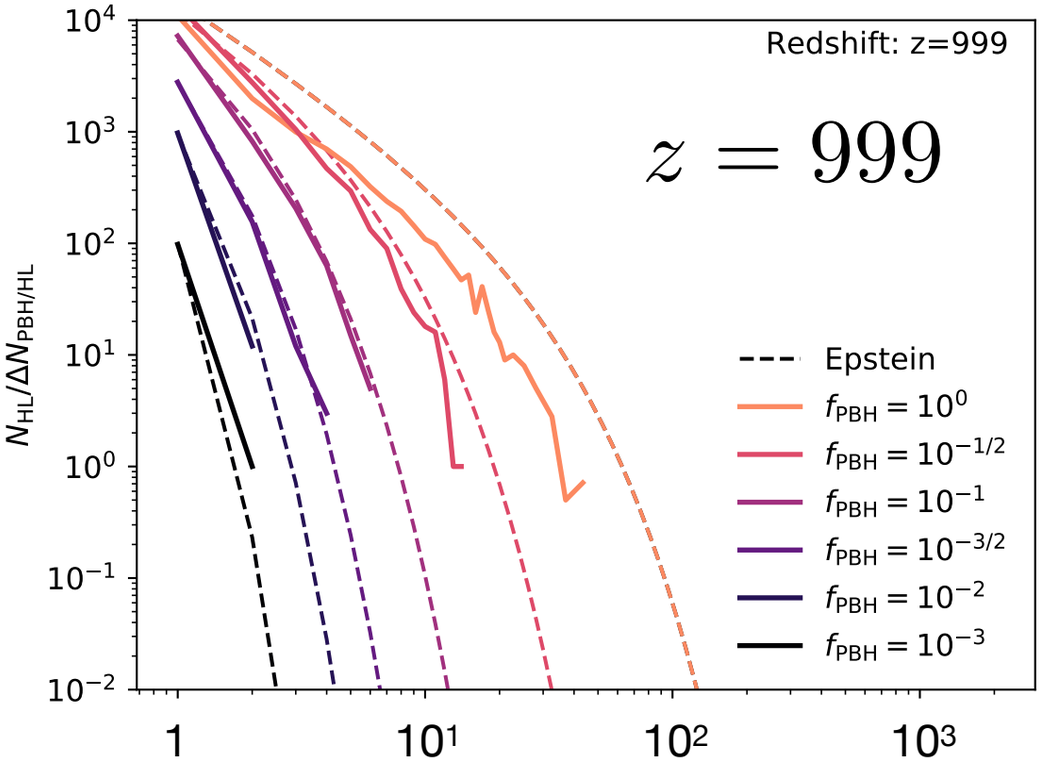

decreasing f_{PBH}

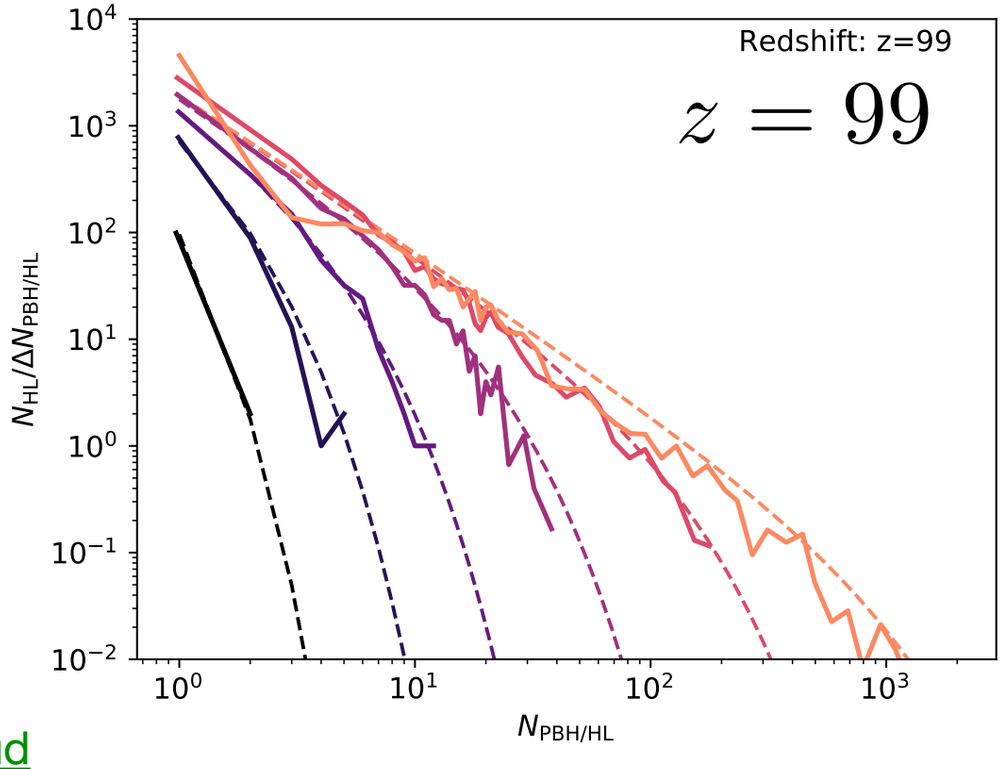

Inman & Ali-Haïmoud

Evolution of PBH clusters (and in particular PBH binaries) through to the present day is a challenging open problem. e.g. Jedamzik; Trashorras et al….

Clusters containing $\lesssim 10^3$ PBHs will evaporate by present day. Afshordi, Macdonald & Spergel; Jedamzik

Effect of clusters on LMC microlensing constraints

Gorton & Green (see also Petaĉ, Lavalle & Jedamzik)

For PBHs formed from collapse of density perturbations during radiation, clusters are sufficiently extended that PBHs lens individually (separation of PBHs $\gg R_E$).

Microlensing from a single cluster:

looking down on line of sight

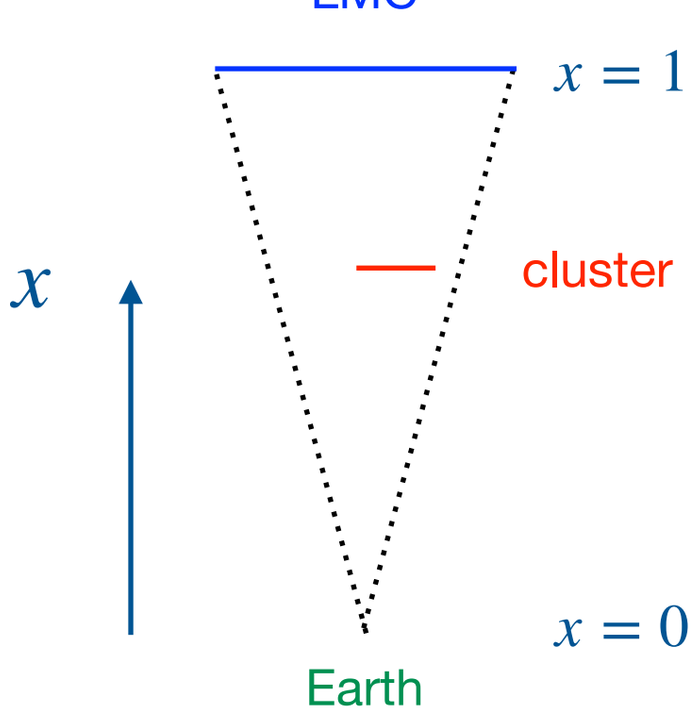

x = fractional line of sight dist

looking along line of sight

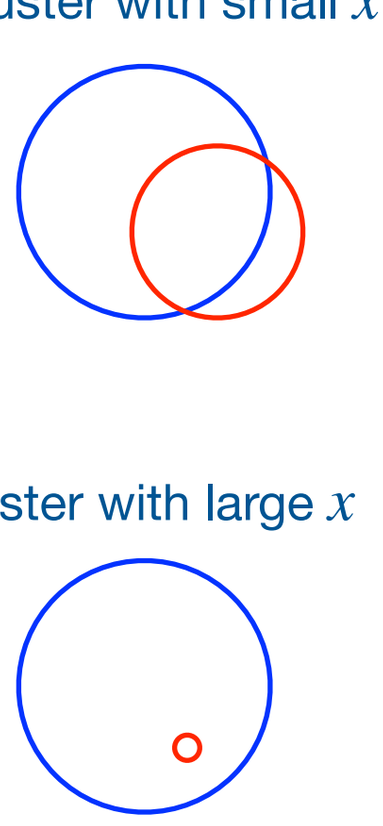

probability of finding a cluster at line of sight distance x is proportional to cross sectional area of 'cone' to LMC $\propto x^2$

all the PBHs in a given cluster cause events with the same duration:

$$\hat{t} = \frac{2R_{\rm E}(x)}{v} \propto [x(1-x)]^{1/2}$$

rate at which cluster causes microlensing events is proportional to solid angle subtended by cluster times Einstein radius:

$$\propto \frac{[x(1-x)]^{1/2}}{x^2}$$

Close clusters (small x) are rare, but if one intersects the line of sight if produces short duration events at a high rate.

LMC microlensing differential event rate for clustered DM and standard smooth DM

all DM in clusters containing $N_{\rm cl} = 10^6$ PBHs

n.b. extremely unrealistic!

$M_{\rm PBH} = 1 M_\odot$

$M_{\rm PBH} = 10 M_\odot$

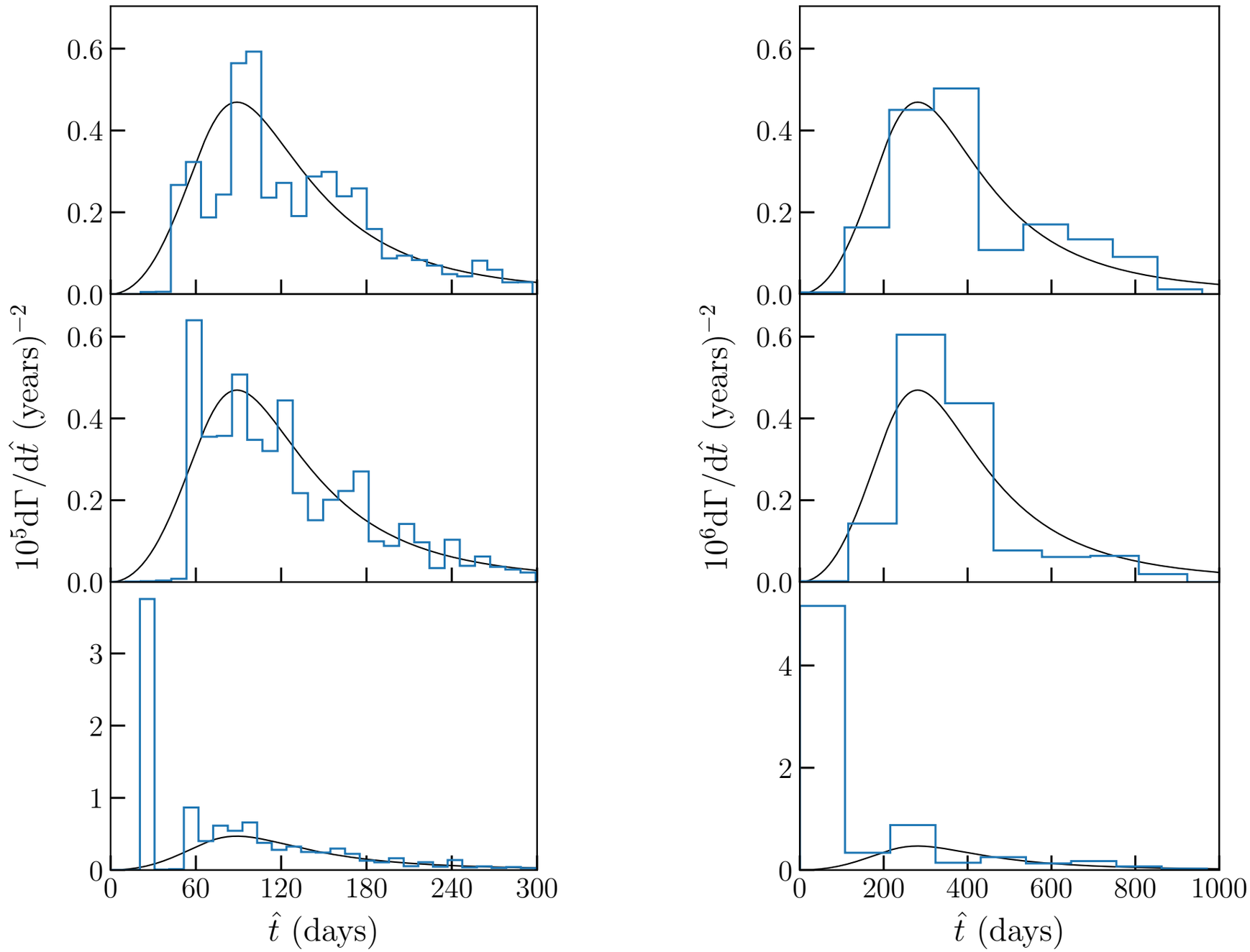

Typical realisations

No close cluster.
Deficit of short duration events.

Rare realisation

Close cluster.
Excess of short duration events.

Probability distribution of number of events in a long-duration microlensing survey if all of the DM is in PBHs clusters containing $N_{\rm cl}$ PBHs with mass $M_{\rm PBH} = 10^3 M_\odot$

Typical realisations

No close cluster.
Deficit of events.

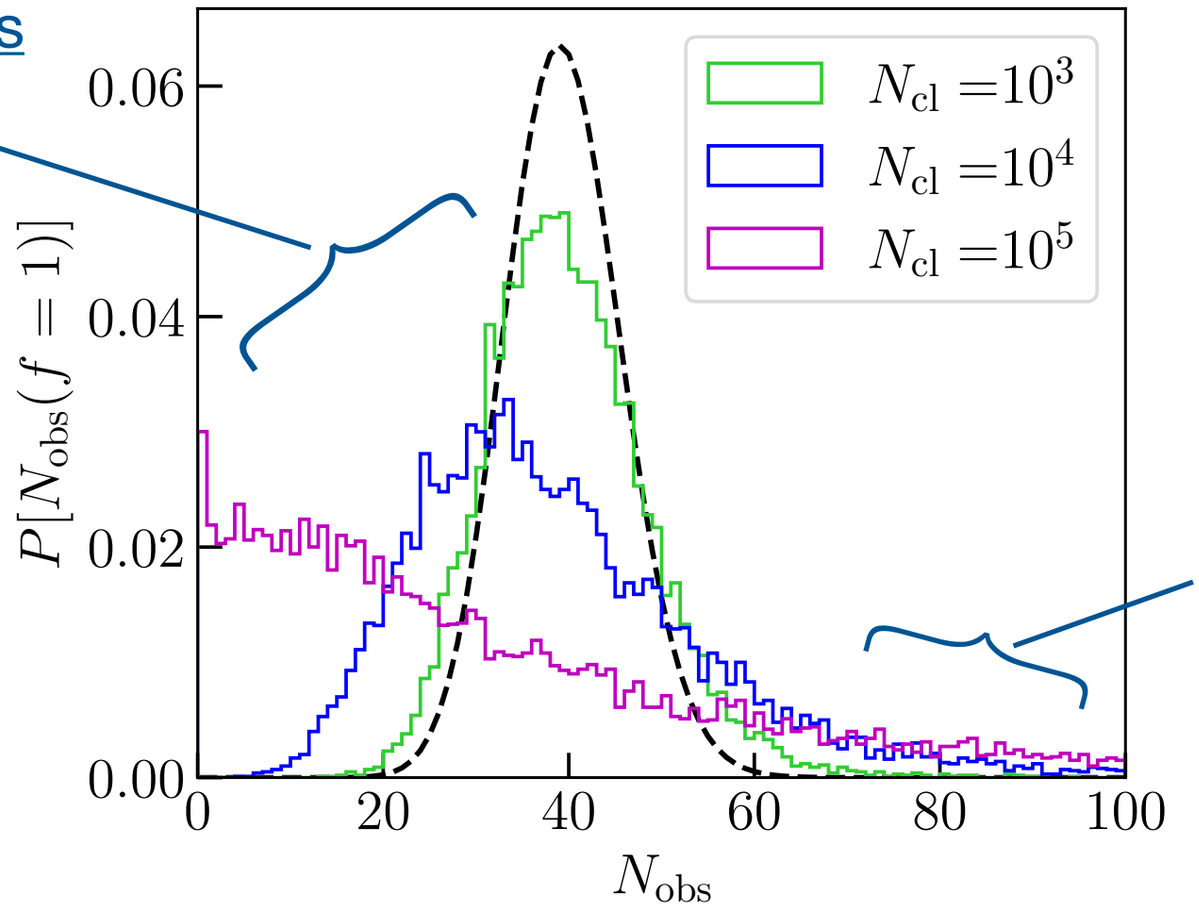

Rare realisations

Close cluster.
Excess of events.

Change in constraints is negligible apart (possibly) from at largest $M_{\rm PBH}$ probed by stellar microlensing (**if** all of the DM is in extended PBH clusters containing $N_{\rm cl} = 10^3$ PBHs with mass $M_{\rm PBH} = 10^3 M_\odot$ constraint on $f_{\rm PBH}$ from long-duration microlensing survey weakens by ~10%). Petaĉ, Lavalle & Jedamzik; Gorton & Green.

Compact clusters

Local non-Gaussianity leads to enhanced clustering. Young & Byrnes; Animali & Vennin

If clusters are sufficiently compact entire cluster (rather than individual PBHs) acts as single lens and microlensing constraints shifted to lower masses Calcino, Garcia-Bellido & Davis however other constraints (e.g. Lyman-α) are tightened. de Luca et al.

two-point correlator: $\xi_{\rm PBH} \approx \xi_0 \quad \text{for} \quad r \lesssim r_{\rm cl}$

excluded by microlensing, Lyman-α

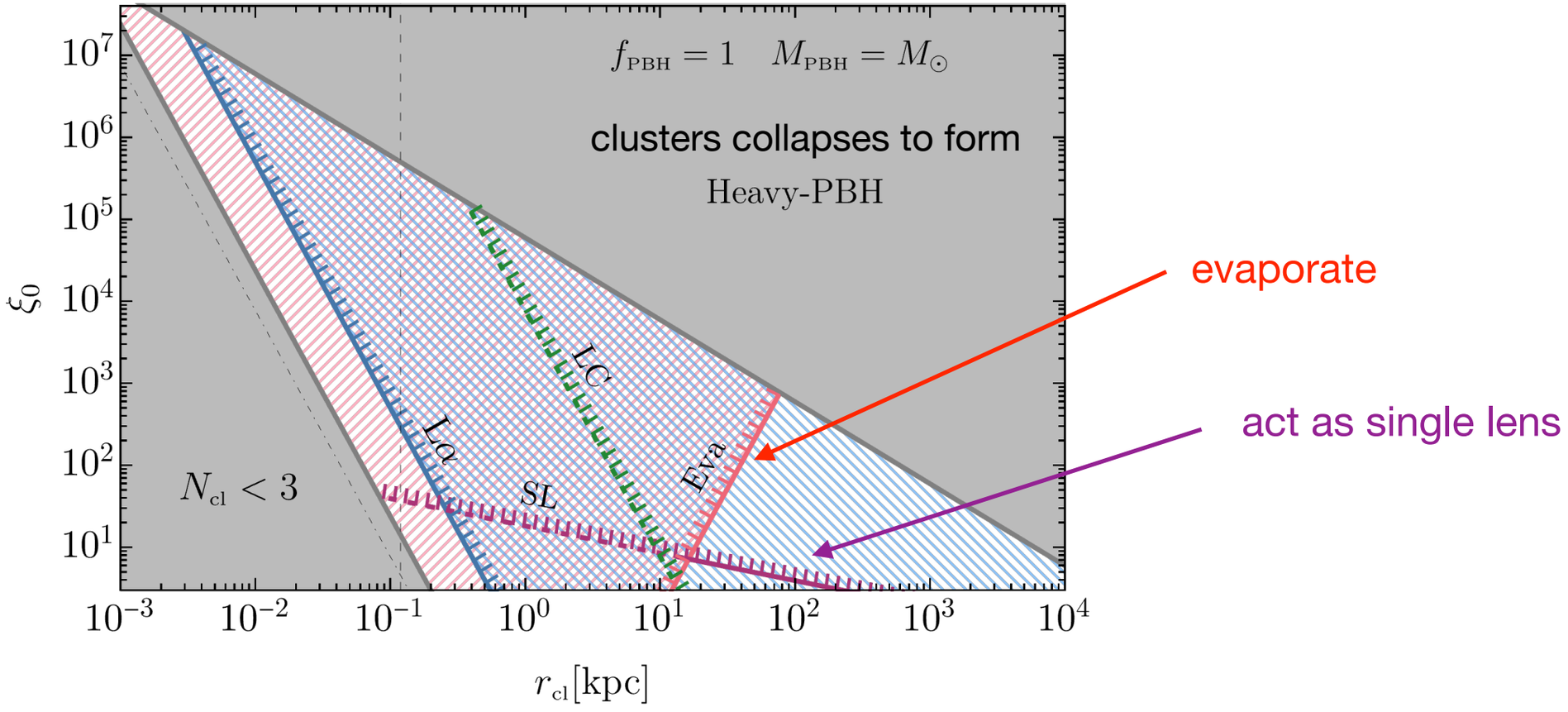

de Luca et al.